GENE DELIVERY

Journal of Controlled Release 159 (2012) 222–231

Contents lists available at SciVerse ScienceDirect

Journal of Controlled Release

journal homepage: www.elsevier.com/locate/jconrel

Development of a recombinant fusion protein based on the dynein light chain LC8 for non-viral gene delivery

Marcelo A.S. Toledo [a], Richard Janissen [c], Marianna T.P. Favaro [a], Mônica A. Cotta [c], Gabriel A. Monteiro [d], Duarte Miguel F. Prazeres [d], Anete P. Souza [a], Adriano R. Azzoni [a,b,*]

[a] Laboratory of Genetics and Molecular Analysis, Molecular Biology and Genetic Engineering Center, State University of Campinas, Campinas, SP, Brazil
[b] Chemical Engineering Department, Escola Politécnica, University of São Paulo, São Paulo, SP, Brazil
[c] Applied Physics Institut "Gleb Wataghin", State University of Campinas, Campinas, SP, Brazil
[d] IBB-Institute for Biotechnology and Bioengineering, Centre for Biological and Chemical Engineering, Instituto Superior Técnico, 1049–001, Lisboa, Portugal

ARTICLE INFO

Article history:
Received 21 September 2011
Accepted 12 January 2012
Available online 20 January 2012

Keywords:
Non-viral gene delivery
LC8 dynein light chain
Microtubules
DNA vaccines
Gene therapy

ABSTRACT

The low efficiency of gene transfer is a recurrent problem in DNA vaccine development and gene therapy studies using non-viral vectors such as plasmid DNA (pDNA). This is mainly due to the fact that during their traffic to the target cell's nuclei, plasmid vectors must overcome a series of physical, enzymatic and diffusional barriers. The main objective of this work is the development of recombinant proteins specifically designed for pDNA delivery, which take advantage of molecular motors like dynein, for the transport of cargos from the periphery to the centrosome of mammalian cells. A DNA binding sequence was fused to the N-terminus of the recombinant human dynein light chain LC8. Expression studies indicated that the fusion protein was correctly expressed in soluble form using *E. coli* BL21(DE3) strain. As expected, gel permeation assays found the purified protein mainly present as dimers, the functional oligomeric state of LC8. Gel retardation assays and atomic force microscopy proved the ability of the fusion protein to interact and condense pDNA. Zeta potential measurements indicated that LC8 with DNA binding domain (LD4) has an enhanced capacity to interact and condense pDNA, generating positively charged complexes. Transfection of cultured HeLa cells confirmed the ability of the LD4 to facilitate pDNA uptake and indicate the involvement of the retrograde transport in the intracellular trafficking of pDNA:LD4 complexes. Finally, cytotoxicity studies demonstrated a very low toxicity of the fusion protein vector, indicating the potential for *in vivo* applications. The study presented here is part of an effort to develop new modular shuttle proteins able to take advantage of strategies used by viruses to infect mammalian cells, aiming to provide new tools for gene therapy and DNA vaccination studies.

1. Introduction

Gene therapy and DNA vaccination protocols demand efficient and safe mechanisms to deliver therapeutic genetic material to the patient cell nucleus. So far, viral-based vectors have been preferred as delivery vehicles since they are naturally efficient in receptor-mediated recognition and cell internalization, endosomal escape, nuclear transport and DNA integration [1,2]. Nevertheless, the use of viruses as gene delivery systems continues to rise safety concerns and the future development of viral gene therapy continue to generate intense scientific debates [2,3]. The alternative approach, non-viral vectors, is considered safer and has been also attracting significant attention of the scientific community. Efforts have been made to increase the delivery efficiency of non-viral vectors, including the creation of sophisticated vehicles able to mimic some of the viral properties regarding both size and biological properties [2]. These vectors are called "artificial viruses" and include polymeric constructs [4–6], protein-only shells and virus-like particles [4]. Among the properties of these vectors are the ability to condense and protect DNA from nuclease degradation, low systemic and cellular toxicity, membrane crossing abilities, and steady expression of the therapeutic gene [7]. However, the inability of these vectors to efficiently traverse the target cell cytoplasm and reach the nucleus has largely been overlooked [8]. It has been also reported that non viral vectors face several extra- and intracellular barriers before DNA can be delivered to the cell's nucleus [9] and that cytosolic proteins may bind to the delivery complex acting as another barrier [10].

The majority of the non-viral vectors studied so far rely on passive diffusion or non specific transport for trafficking within the cytoplasm, and this limited mobility represents a significant barrier to gene delivery [11]. Since it has been shown that diffusion of DNA

* Corresponding author at: Chemical Engineering Department, Escola Politécnica da USP, Av. Prof. Luciano Gualberto, Trav. 3, No. 380, CEP 05508–900, São Paulo, SP, Brazil. Tel.: +55 11 30912234; fax: +55 11 30912284.
E-mail address: adriano.azzoni@poli.usp.br (A.R. Azzoni).

0168-3659/$ – see front matter © 2012 Elsevier B.V. All rights reserved.
doi:10.1016/j.jconrel.2012.01.011

fragments larger than 2000 base pairs through the crowded cytoplasmic environment is greatly restricted [12], an ideal vector should, like most viruses, include the ability to exploit the host cell machinery to rapidly traverse the cytoplasm. Many authors have suggested that an ideal form to actively transport drugs, including transgenes, from the site of cytoplasmic entry to the nuclear periphery would include recruitment of the minus end-directed motor dynein [8,13–15]. Cytoplasmic dynein is a multisubunit protein complex (~1.2 MDa) composed of two heavy chains (~530 kDa) responsible for microtubule attachment and ATP hydrolysis [16], two 74-kDa intermediate chains (IC74), four light intermediate chains (52–61 kDa), and several light chains (10–25 kDa) which are responsible for cargo attachment to the dynein motor complex and hence, its transport through the cytosol toward the nucleus [17,18]. However, so far no successful strategies to exploit motor proteins' retrograde transport for efficient gene delivery have been demonstrated. In an attempt to design synthetic gene carriers that display dynein-binding peptides for enhanced intracellular transport, Bergen and Pun (2007) studied the use of a peptide that binds to the dynein light chain LC8 subunit, as the first potential dynein-binding peptide [8]. It was demonstrated that, while the peptide readily bound free LC8, it could not bind to dynein-associated LC8, emphasizing the need to identify or design peptides that could mediate binding to the intact dynein motor complex. More recently, Moseley and collaborators (2010) reported that protein transduction can be enhanced by attachment to a dynein light chain association sequence [15]. These sequences were able to enhance nuclear accumulation of GFP-fusion proteins, with dependence on the LC8/microtubule (MT) network. This work provided the first successful evidence that dynein/MT-association can be exploited for DNA or drug delivery approaches.

Here, we propose the use of the dynein light chain LC8 itself as a cargo adaptor for plasmid delivery into mammalian cells, taking advantage of the dynein retrograde transport *via* the MT network. LC8, also called DYNLL1, is a small (10 kDa) and highly conserved globular protein reported as an essential component of the dynein and myosin V molecular motors [19,20]. The LC8 binds as a dimer directly to specific sites on the dynein intermediate chain IC74 or myosin V heavy chain, while some studies indicate additional roles for LC8 in multiple protein complexes unrelated to the motor proteins such as p53-binding protein 1 [21], neuronal nitric oxide synthase [22], the proapoptotic member of the Bcl-2 family proteins Bim and Bmf [23,24], the product of the *Drosophila* swallow gene [25], and a number of proteins with unknown functions [26]. We envision that LC8 could be modified with short DNA-binding sequences, rich in positively charged amino acids, which would interact and condense pDNA and facilitate its transport toward the nucleus periphery *via* interaction with the dynein complex. Finally, the work presented here intends to generate new information on plasmid delivery and presents a new strategy for the development of modular non-viral vectors potentially useful for gene therapy and DNA vaccination.

2. Materials and methods

2.1. Plasmid DNA vector

In the present study, a plasmid DNA model named pVAX1-Luc was constructed based on the previously reported pVAX1-GFP plasmid [27]. Using XbaI and EcoRI restriction endonucleases, the sequence coding for GFP was replaced by the luciferase gene obtained from the pGL3-Luc control vector (Promega) using the same restriction enzymes. The success of the reporter gene replacement was confirmed by the expression of the reporter enzyme after transfection of HeLa cells, as described in this work. Purification of the pVAX1-Luc plasmid used in all transfection studies was performed as described by Freitas and co-workers [28].

2.2. DNA binding domains design

The fusion protein DNA binding domains were designed based on the scientific literature available [2,29] for peptides and protein domains with high DNA binding and condensing capacity. We designed four domains to be cloned upstream of human dynein light chain LC8: DNAb1, WRRRGHGKKK; DNAb2, WRRRGFGKKK; DNAb3, WRRRGHGRRR; and DNAb4, WRRRGFGRRR. The corresponding single strand oligonucleotides were synthesized with optimized codons for *E. coli* expression and annealed before cloning. The DNA binding domains were cloned in the *NdeI* and *BamHI* sites in the pET28a expression vector (Novagen, Darmstadt, Germany). The clones containing the DNA binding domains were further used for LC8 cloning in the *BamHI* and *XhoI* restriction sites. In this work we define as LD4 the recombinant human LC8 fused to the DNA binding domain 4 (DNAb4), described above.

2.3. Recombinant proteins expression and purification

The human dynein light chain LC8 was amplified from HeLa cDNA with specific primers (forward:5′-ATAGGATCCATGTGCGACCGAAAG-3′, reverse: 5′ATACTCGAG TTAACCAGATTTGAACAGAAGA-3′) and cloned into pET28a with and without DNA binding domains previously cloned at the N-terminal. Recombinant LC8 with or without DNA binding domains were expressed in *E. coli* BL21(DE3). Briefly, cells were grown in 1 L LB medium at 37 °C, 300 rpm and up to an optical density of 0.8 AU (600 nm). Protein expression was induced with 5.6 mM lactose or 0.2 mM IPTG (isopropyl-β-D-thiogalactopyranoside) for further 12 h at 25 °C, 200 rpm. After centrifugation, the cell pellet was suspended in 50 mM sodium phosphate pH 8.0, 500 mM NaCl, 0.1 mM EDTA, 15 mM β-mercaptoethanol and 1 mM PMSF (phenylmethylsulfonyl fluoride). Cell lysis was performed by sonication and the recombinant LC8 was purified by a single Ni-NTA affinity chromatography step. This method was successfully used to purify recombinant LC8 with and without the four different DNA binding domains.

For *in vitro* interaction of recombinant dynein light chain LC8 and LD4 with human dynein intermediate chain DYNIC2 its N-terminal domain (the first 300 amino acids) and the dynein light chain TcTex were cloned using the same methodology as described for LC8. The DYNIC2 domain was amplified with specific primers from HeLa cDNA and cloned into pET28a using *NdeI* and *BamHI* restriction sites (forward, 5′-ATTCATATGATGTCAGACAAAAGTGAATT-3′, reverse, 5′-ATTGGATCCTTAGTTATAGGAAGCCAC-3′). The TcTex light chain was inserted in *BamHI* and *XhoI* restriction sites (forward, 5′-ATAGGATCCATGGAGGAGTACCATCG-3′, reverse, 5′-ATACTCGAGTTAAAGAACAATAGCAATGG-3′). Both recombinant proteins were expressed in *E. coli* BL21 (DE3) Rosetta strain. The expression of the N-terminal DYNIC2 was induced with 0.2 mM IPTG at 20 °C and 200 rpm for 12 h. For all recombinant proteins, purity was evaluated by SDS-PAGE and concentration was measured by absorbance at 280 nm.

2.4. Circular dichroism studies

Circular dichroism (CD) spectra of the purified recombinant proteins were obtained using a Jasco J-810 Spectropolarimeter dichrograph (Japan Spectroscopic, Tokyo, Japan). The far-UV CD spectra were generated at 20 °C using 10–20 μM of each protein in 10 mM sodium phosphate buffer pH 8.0. The assays were carried out using a quartz cuvette with a 1 mm path length. Ten accumulations within the 185–260 nm range at a rate of 50 nm/min were recorded. Data was processed using OriginLab 8.0 software.

2.5. Size exclusion chromatography

To assess the oligomeric state of purified LC8 with and without DNA binding domains, size exclusion chromatography was performed using a Superdex 200 GL10/300 or Superdex 75 GL10/300 prepacked column

(GE Healthcare, Uppsala, Sweden). After equilibration of the column with extraction buffer or PBS (8.0 g NaCl, 0.2 g KCl, 1.4 g Na_2HPO_4, 0.24 g $KH2PO_4$, pH 7.4 per liter), oxidized and reduced (10 mM DTT) samples (250 μl) were loaded at a flow rate of 0.75 ml/min. The calibration curve was prepared using High and Low molecular calibration kits (GE Healthcare). Gel permeation chromatography was also used to evaluate LC8-TcTex-Intermediate chain complex formation.

2.6. In vitro interaction of recombinant dynein light chains LC8 and TcTex with dynein intermediate chain 2, isoform C

In order to evaluate the ability of recombinant LC8 and LD4 to interact *in vitro* with the human dynein intermediate chain DYNIC2, isoform C, the N-terminal of this protein (first 300 amino acids) was cloned, expressed and purified as described. We also used in this assay the TcTex light chain since its presence in the complex may enhance the interaction between LC8 and the intermediate chain, as discussed in the Results and discussion section. LC8 (19.2 μM) or LD4 (8.9 μM) and TcTex (6.3 μM) light chains were incubated with purified intermediate chain domain, IC_{DOM} (7.23 μM), at 8 °C for 20 h under reducing conditions (10 mM DTT). The purified proteins were used immediately after purification procedure and complex was formed in 50 mM sodium phosphate pH 8.0, 500 mM NaCl, 0.1 mM EDTA and approximately 200 mM imidazole. Complex formation was evaluated by gel permeation chromatography using a Superdex 75 GL10/300 prepacked column (GE Healthcare, Uppsala, Sweden) and collected samples corresponding to the complex elution peaks were concentrated (10-fold concentration) using a Amicon Ultra Centrifugal Filter (3 kDa) (Millipore, Ireland) and visualized by SDS-PAGE.

2.7. Evaluation of DNA-protein interaction by gel retardation assay

To evaluate the ability of LC8, LC8 with different DNA binding domains and protamine to interact and condense pDNA, we performed a gel retardation assay. Proteins were dialyzed in PBS (protamine sulfate powder was ressuspended in PBS) and incubated with 250 ng of pVAX-Luc vector (previously in PBS) at different pDNA:protein molar ratios (1:400, 1:800, 1:1000, 1:2000, 1:4000 and 1:8000) in a final volume of 50 μL. The samples were incubated at room temperature for 1 h following by the addition of 50 μL of non supplemented F-12 media and additional incubation for 20 min. Samples were run in a 0.8% agarose gel and visualized by ethidium bromide staining.

2.8. Zeta potential and particle size assays

Zeta potential measurements were performed to comparatively evaluate the surface charge of complexes formed by pDNA:LC8 and pDNA:LD4. Complexes were formed as described for gel retardation assay but without F-12 media addition and using the same pDNA:protein molar ratios. Each sample was measured in triplicate using Zetasizer 3000 (Malvern, England). Particle size measurements were performed to evaluate the behavior of different complexes regarding its size along time. pDNA:protamine (pDNA:protein molar ratio of 1:8000) and pDNA:LD4 (pDNA:protein molar ratio of 1:100 and 1:8000) complexes with and without Lipofectamine™ and pDNA:Lipofectamine™ complexes were formed by 1.0 μg of pDNA and the corresponding amount of protein in a final volume of 800 μL. When indicated, 1.5 μL of Lipofectamine™ was added to the complex. Each sample was submitted to multiple readings during a 60 min period. Particle diameter was plotted against time for each sample.

2.9. Atomic force microscopy (AFM)

Plasmid DNA:protein complexes at different molar ratios (1:400, 1:1000 e 1:2000 for LC8 and 1:100, 1:200 e 1:500 for LD4) were prepared in 10 mM Tris–HCl buffer pH 7.4 in a final DNA concentration of 600 pg/μl by incubation at room temperature for 1 h. After complex formation, a final concentration of 5 mM $MgCl_2$ was added to each sample and 60 μl of the solution was physisorbed for 1 min on freshly cleaved muscovite mica (Ted Pela, California, USA). After adsorption, the surface was washed for 10 s in ultrapure water and dried in a weak nitrogen stream. The AFM imaging was performed in air a room temperature in acoustic mode at a scanning speed of 300 nm/s with an Agilent 5500 (Agilent, Santa Barbara, USA) using commercial silicon cantilevers (MicroMash, NSC-14/ALBS) with a tip radius of approximately 10–20 nm. The topography images were treated using the Open-Source software Gwyddion (www.gwyddion.net).

2.10. Culture and transfection of HeLa cells

HeLa cells were grown in F-12 (Ham) nutrient mixture (Gibco, UK) containing 10% (v/v) fetal bovine serum (growth medium, Gibco, UK). All cell cultures were performed in 75 cm^2 culture flasks and incubated in 5% CO_2 humidified environment at 37 °C. Following growth up to confluence, cells were trypsinized and seeded in 24 well culture plates (5×10^4 cells per well). The cells were incubated for 48 h (to a 70% confluence) and then transfected with pDNA:protein complexes formed as described for gel retardation assays and using the same molar ratios. When indicated, transfection was carried out using the Lipofectamine 2000™ reagent (Invitrogen, USA) according to the manufacturer instructions (1.0 μg pDNA plus 1.5 μL reagent in 100 μL of medium per well), protamine sulfate (Sigma Aldrich, Germany) or PEI (polyethylenimine, branched, MW ~25,000) (Sigma Aldrich, Germany). The medium containing the transfection solution remained on the cell containing wells for 6 h and was then replaced by regular growth medium. Cells were collected after 24 h post-transfection for determination of luciferase activity using the luciferase Assay System (Promega, USA), following the manufacturer's instructions. Luminescence intensity was normalized against protein concentration in each transfection sample, as determined by the Micro BCA Protein Assay Kit (Thermo Scientific, USA).

To evaluate the contribution of the microtubule network and actin filaments in the intracellular trafficking of the complexes, cells were pre-incubated for 2 h with nocodazole (25 μM) or cytochalasin D (25 μM) for microtubule and actin filaments disruption, respectively. Both drugs were dissolved in DMSO and an equal volume of drug-free DMSO was used as control (0.5% for cytochalasin D and 0.4% for nocodazole). Transfections in the presence of chloroquine were performed to evaluate the contribution of lysosomal degradation of protein-pDNA complexes. Cells were pre-incubated for 4 h with chloroquine (100 μM). For all assays with the mentioned drugs, pre-treated cells were incubated afterwards in the presence of the different complexes for 4 h, when the medium was replaced by freshly growing medium. After 24 h, cells were collected and the luciferase activity was assayed as described above.

Cytotoxicity assays of delivery vectors studied in the present work were performed using Cell Proliferation Reagent WST-1 (Roche Applied Science, USA) following manufacturer's instructions. Briefly, HeLa cells were grown on 96 wells plates to a confluence of 70%. Transfection was performed as described before with pDNA:protein complexes (molar ratio of 1:8000) with and without Lipofectamine™, with pDNA:Lipofectamine™, and also with naked pDNA as control. Finally, 10 μL of the WST-1 reagent was added to each well, and cells were further incubated for 2 h. Absorbance was read after 60 s agitation at 440 nm using a Spectramax 384 Plus UV/VIS Microplate Reader (Molecular Devices, USA).

3. Results and discussion

3.1. Recombinant human dynein light chain LC8 was successfully produced with N-terminal DNA binding domains

Using the methodology described above we were able to produce recombinant LC8 and recombinant LC8 fused to DNA binding domains

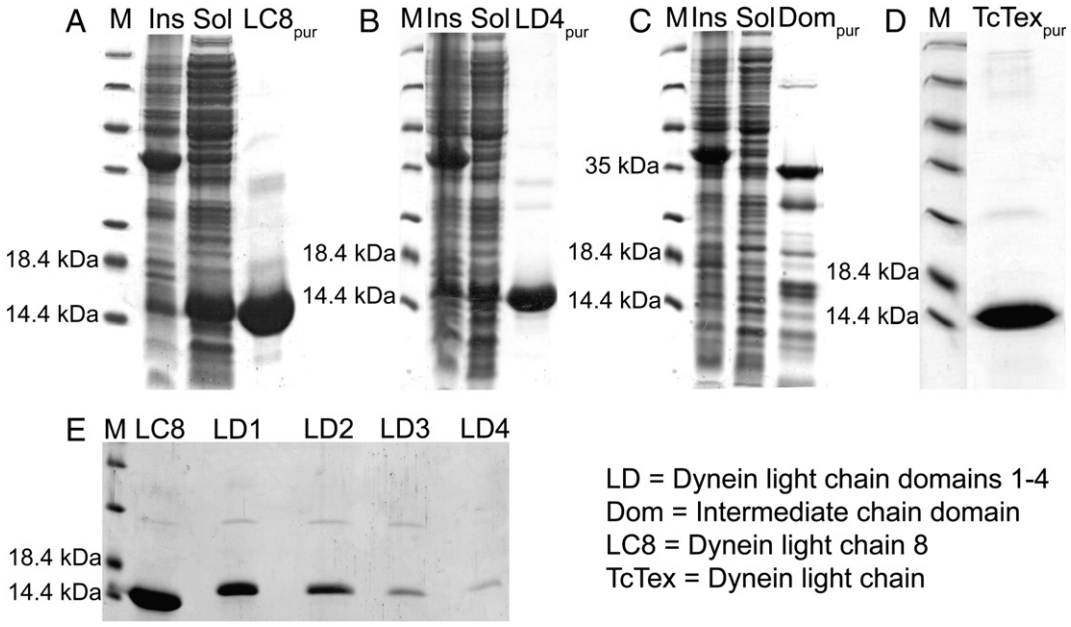

Fig. 1. SDS-PAGE analysis of purified recombinant proteins used in the present study. A: Purified LC8. B: Purified LD4. C: Purified intermediate chain N-terminal domain. D: Purified TcTex. E: LC8 and LC8 with the four different DNA binding domains at the N-terminal after dialysis against PBS. M: Broad Range molecular weight marker (Fermentas). Ins: Insoluble fraction after cell lysis. Sol: Soluble fraction after cell lysis. $LC8_{pur}$: purified LC8. $LD4_{pur}$: purified LD4. Dom_{pur}: purified N-terminal domain of DYNIC2 intermediate chain. $TcTex_{pur}$: purified TcTex. LC8, LD1,LD2,LD3,LD4: LC8 without and with each DNA binding domain.

(DNAb1, DNAb2, DNAb3 and DNAb4), all proteins efficiently expressed in *E. coli* BL21(DE3) strain. All constructs were obtained in the soluble fraction after cell disruption and purified by a single Ni-NTA affinity chromatography step (Fig. 1). Circular dichroism analysis of the secondary structures of the proteins showed that addition of the DNA binding domains had little effect on the secondary fold of LC8 probably due to the addition of the domain to its N-terminal (Fig. 2 and Supplementary Data). The oligomeric state of LC8 and LC8 fused with DNAb4 (LD4) was evaluated in phosphate saline buffer (PBS) by gel permeation chromatography under reduced and non reduced conditions. We could observe that the human LC8 is dimeric under reducing conditions, as reported for the *Drosophila* homologue [30], and appears as a tetramer under non reducing conditions (results not shown). The LD4 presented a higher propensity to aggregate under low ionic strength (such as in PBS), as judged by the fact that a significant portion of the purified protein precipitated during dialysis against PBS, even under reducing conditions. Gel permeation chromatography shows that LD4 in PBS under reducing and non reducing conditions is polidispersed in diverse oligomeric subpopulations. However, analysis of small angle X-ray scattering (SAXS) data for Lc8 and LD4, collected in 50 mM sodium phosphate, 500 mM NaCl, 0.1 mM EDTA and 500 mM Imidazole, allowed us to assume that the recombinant proteins were folded in solution under reducing conditions. A bell shaped Kratky plot was observed, which is characteristic of folded proteins (Supplementary Data). Therefore, the observed aggregation for LD4 may be due to the relative low ionic strength of PBS. In summary, our results indicate that the recombinant LC8 and its variations with different DNA binding domains were successfully and correctly expressed and purified (Fig. 1) allowing us to proceed with pDNA interaction and transfection assays. It is noteworthy that LD4 (as well with other DNA binding domains), despite appearing as a population of aggregates in gel permeation assays, was successfully used in pDNA condensation assays, indicating that upon DNA addition, the protein aggregates were disrupted allowing protein interaction with the pDNA.

3.2. Recombinant LC8 and LD4 are able to interact in vitro with human dynein intermediate chain

The human LC8 dynein light chain interacts with the dynein intermediate chain and some other proteins not related to the dynein motor complex as mentioned before (see Introduction). Additionally, the interaction between LC8, TcTex and the intermediate chain IC74 is well characterized for the *Drosophila* homologues. In a recent work, Hall and collaborators (2009) showed that when one of the light chains (LC8 or TcTex) is previously bound to the intermediate chain IC74, the binding of the second light chain is enhanced by 50-fold [31]. In the context of the gene delivery mechanism envisioned in

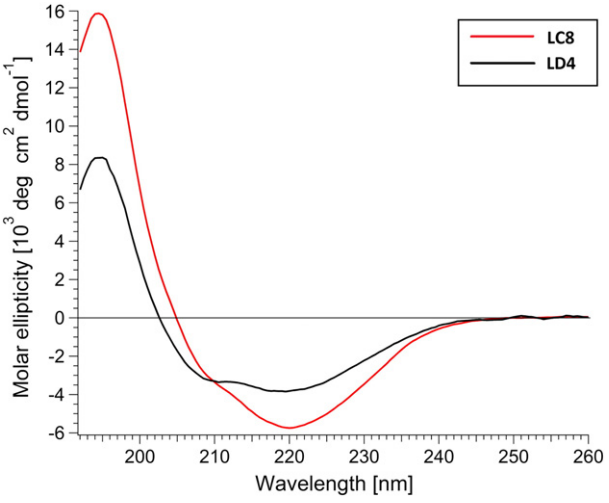

Fig. 2. Circular dichroism curves for dynein light chain LC8 and for LC8 fused with DNA binding domain 4. LC8: LC8 dynein light chain. LD4: LC8 dynein light chain fused with DNAb4 binding domain. Little variation between the spectra can be observed probably due to the addition of the DNA binding domain.

the present work, the recombinant dynein light chain LC8, whether fused or not to DNA binding domains, should be able to interact with the dynein machinery. Thus, in order to analyze the functionality of recombinant LC8 and LD4, we assayed their interaction with the N-terminal domain (300 first amino acids) of the human dynein intermediate chain 2, isoform C (DYNIC2), in combination with TcTex dynein light chain. We could observe that both, LC8 and LD4 were able to interact *in vitro* with dynein intermediate chain by gel permeation chromatography and subsequent SDS-PAGE analysis of the eluted peak (Fig. 3). This result shows that the recombinant LC8 light chain, with or without the N-terminal DNA binding domain retains its functionality once it is able to interact with human intermediate chain *in vitro*.

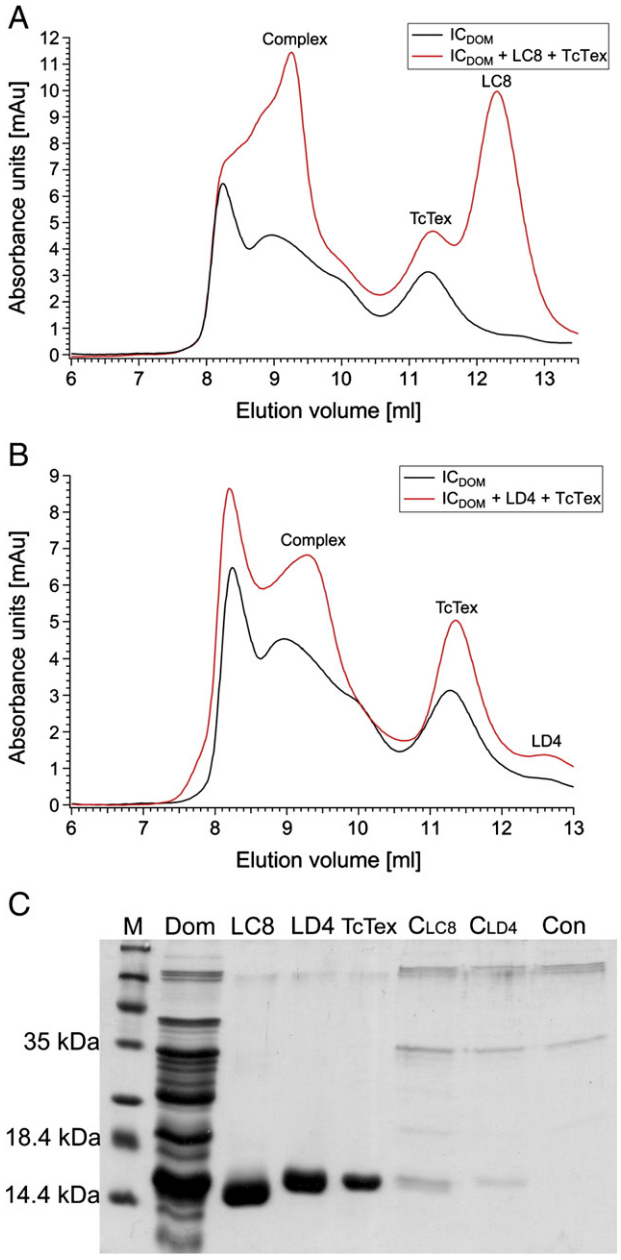

Fig. 3. Interaction of recombinant LC8 and LC8 with DNA binding 4 with the N-terminal domain of DYNIC2 and with the dynein Light Chain Tctex. A: Gel permeation chromatography elution curves for LC8-DYNIC2-TcTex. B: Gel permeation chromatography elution curves for LD4-DYNIC2-TcTex. C: SDS-PAGE 15% for elution samples from gel permeation chromatography showing that DYNIC2 and Light Chains are eluted together indicating interaction. Dom: purified N-terminal domain of Intermediate Chain (premature translation end can be observed for this protein). LC8: purified LC8. LD4: purified LD4. TcTex: purified TcTex. C_{LC8}: elution peak collected at 9 ml and concentrated 10 fold for the LC8-DYNIC2-TcTex complex. C_{LD4}: elution peak collected at 9 ml and concentrated 10-fold for the LD4-DYNIC2-TcTex complex. Con: Control experiment, elution peak collected at 9 ml and concentrated 10-fold for DYNIC2 alone.

3.3. Addition of DNA binding domains at the N-terminal of LC8 light chain leads to enhanced interaction and condensation of plasmid DNA

A gel retardation assay was performed to evaluate the effect of DNA binding domains on the LC8 ability to interact and condense pDNA. We tested the same gradient of DNA:protein molar ratio for all DNA binding constructs, for LC8 alone and used protamine as control. Despite being non quantitative, this assay clearly shows an enhanced capacity of LC8 with DNA binding domains to interact and condense pDNA when compared to LC8 alone or to protamine (Fig. 4). At low pDNA:protein molar ratios (1:400), shifted bands can be observed for all constructs with DNA binding domains whereas only at higher molar ratios (1:2000) some shift can be observed for LC8 alone and for protamine. In addition, at higher molar ratios (1:4000), uncomplexed pDNA can still be observed for LC8 whereas for LC8 with DNA binding domains, all pDNA is complexed and has its migration retarded.

3.4. LC8 with DNA binding domain 4 interacts with pDNA generating positively charged complexes

An efficient vector for gene delivery must mediate the condensation and uptake of the genetic material by the cell. Specifically, the delivery vector must help to overcome the charge incompatibility between the negatively charged cell surfaces and pDNA molecules, by generating complexes with a positive net charge. We thus evaluated the surface charge of complexes formed between pDNA and LC8 or LD4. Zeta potential of pDNA-protein complexes was measured at different pDNA:protein molar ratios (Fig. 5A). The plot of zeta potential against each molar ratio shows that the addition of the DNA binding

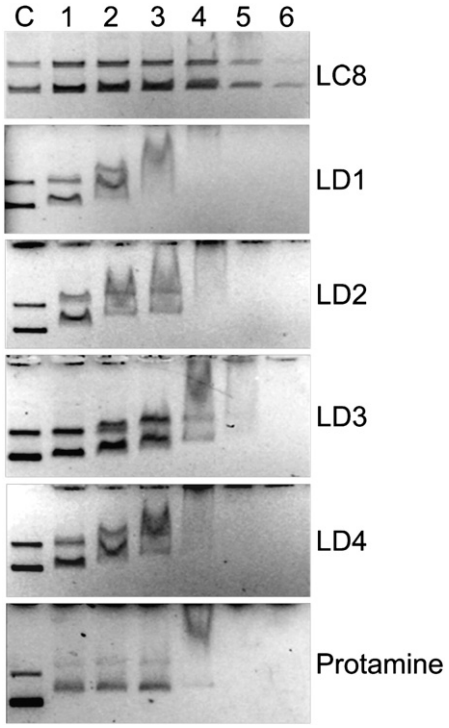

Fig. 4. Protein–DNA interaction analysis by gel retardation assay. The ability of protamine, LC8 and LC8 fused to DNAb1 (LD1), DNAb2 (LD2), DNAb3 (LD3) and DNAb4 (LD4) binding domains to interact and condense plasmid DNA was analyzed by a gel retardation assay. Six pDNA:protein molar ratios were used (lanes 1 to 6): 1:400, 1:800, 1:1000, 1:2000, 1:4000 and 1:8000. C: control pDNA with no protein.

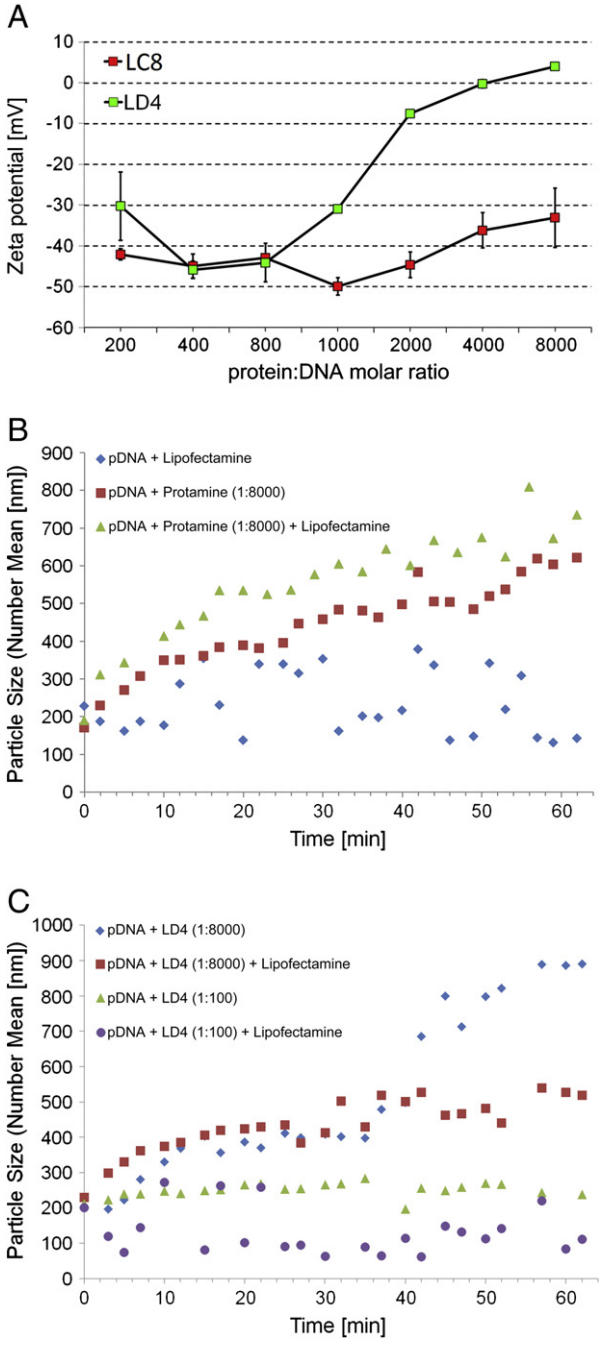

Fig. 5. A: Net surface charge of pDNA complexes formed by LC8 and LC8 fused to DNA binding domain 4 (LD4). The zeta potential of pDNA:protein complexes was measured at seven different molar ratios (1:200, 1:400, 1:800, 1:1000, 1:2000, 1:4000 and 1:8000). LD4 clearly shows higher ability to form positively charged complexes at molar ratios above 1:4000, while LC8 alone generated negatively charged complexes in all conditions tested. B and C: Time course of particle size for the different pDNA:delivery vector complexes studied.

sequence 4 to LC8 enabled the formation of complexes with positive net surface charge when a molar ratio above 1:4000 was used. For complexes formed with LC8 without DNA binding sequence, the net surface charge remained negative in all molar ratios tested.

We also monitored the particle size of pDNA:protamine (1:8000 molar ratio) and pDNA:LD4 (1:8000 and 1:100 molar ratio) with and without Lipofectamine™ and pDNA:Lipofectamine™ complexes during 60 min of incubation at room temperature (Fig. 5B and C). This analysis showed that addition of Lipofectamine™ to pDNA:protein complexes (LD4 or protamine) slightly increased the particle size, especially in the first 40 min of incubation. After that, pDNA:LD4 complexes, in especial, presented a sharp increase in size, probably due to aggregation caused by the lack of electrostatic repulsion, as indicated by the low values of zeta potential. Interestingly, the smallest complex which also showed no significant variation during the analysis was pDNA:LD4 (1:100) with Lipofectamine™. Particle size and particle surface charge are two main factors that dictates internalization of the delivery complex by the cell and is directly correlated to transfection efficiency [32,33]. Thus, by monitoring both variables we are able to correlate and perhaps explain the results found during transfection.

In order to evaluate the pDNA condensation, we performed atomic force microscopy (AFM) assays. The methodology allowed us to visualize the effect of the DNA binding domain 4 on the LC8 light chain affinity for the pDNA molecule. As it can be observed (Fig. 6), LD4 presented enhanced capacity to interact and condense plasmid DNA in contrast to LC8. In excess of both pDNA binding proteins, the pDNA:protein complexes form nearly spherical particles. In comparison, LD4 condenses pDNA to compact particles with sizes in the range of 75 ± 8 nm at lower molar ratios (1:500) than LC8 (1:2000) with size in the range of 101 ± 9 nm. However, it is important to note that the complexes observed by this method were formed at a lower ionic force and different buffer salt (10 mM Tris–HCl buffer) than those shown in gel retardation and Zetasizer experiments (PBS). The excess of salt in PBS buffer strongly affects the AFM imaging procedure. Despite the difference in ionic strength that probably lead to DNA condensation at lower pDNA:protein ratios, the AFM images clearly indicate the effect of the DNA binding domain.

3.5. Transfection experiments demonstrated that LD4 is able to deliver pDNA to HeLa cells

After the interaction tests *in vitro*, we assayed the ability of the fusion protein LD4 to deliver pDNA to HeLa cells in culture. Firstly, we tested complexes formed by pDNA and recombinant LC8 with and without the four different DNA binding domains. These preliminary transfections assays showed that LD4 was the most efficient shuttle protein among all the constructs (results not shown). Therefore, we focused our efforts on LD4, and used LC8 and the arginine rich protamine as controls. The results show that LD4 is more efficient in cell transfection when compared to protamine (Fig. 7A), a well characterized nuclear protein that is known for its ability to condense DNA molecules, facilitate DNA uptake by the cells, and transposition of the nuclear barrier due to presence of a nuclear localization signal [34,35]. LD4 mediated transfection presented a 30-fold higher luciferase expression compared to protamine at the same pDNA:protein molar ratio (1:8000), while LC8 presented even lower efficiency (4-fold lower than protamine). It is noteworthy that pDNA:LD4 (1:8000) complexes formed particles with bigger size than pDNA:protamine (1:8000) complexes as shown by size measurements and a mildly positive surface charge, as shown by Zeta potential measurements. Therefore, the observed enhanced transfection efficiency presented by pDNA:LD4 complexes compared to protamine complexes might be related to an additional property of the recombinant LD4 that facilitates pDNA delivery. Interestingly, when pDNA:LD4 complexes were formed at a molar ratio of 1:16,000, the transfection efficiency dropped 3-fold. It is possible that the decrease in transfection efficiency was caused by protein saturation and formation of bigger complexes by non-specific protein–protein interaction leading to a lower complex uptake by the cell [36].

We also tested multicomponent complexes formed by pDNA and protein (LC8, LD4 and protamine), Lipofectamine™ or PEI (Fig. 7B). Cationic lipids like Lipofectamine™ are known as efficient pDNA delivery vectors in culture cells, enabling the internalization of several thousand pDNA copies per cell during *in vitro* transfection [34]. As expected, binary complexes formed by pDNA and Lipofectamine™

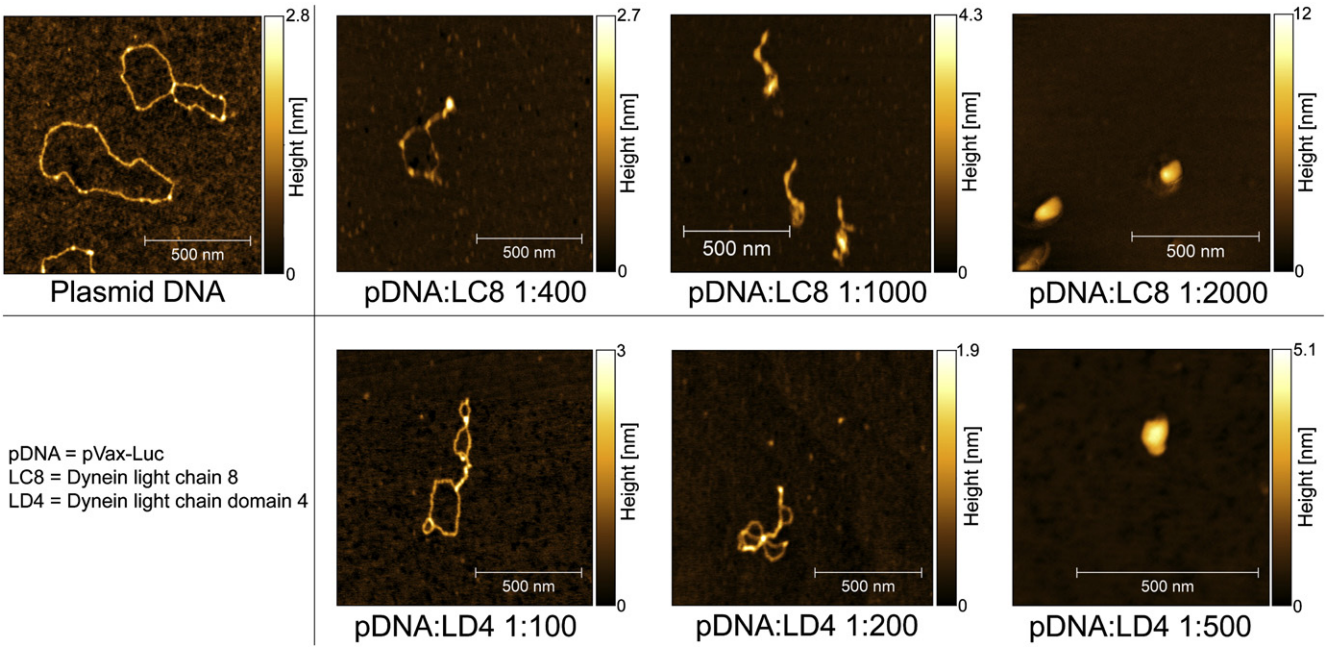

Fig. 6. Visualization of pDNA:LC8 and pDNA:LD4 complexes by atomic force microscopy (AFM). pDNA:protein complexes formed at different molar ratios (1:400,1:1000 and 1:2000 for LC8 and 1:100, 1:200 and 1:500 for LD4) allowed us to visualize the condensation process mediated by the protein. This methodology clearly shows that addition of a DNA binding domain 4 to the LC8 Dynein Light Chain enhanced its ability to interact and condense plasmidial DNA.

promoted higher transfection efficiencies than pDNA:protein complexes (using either LD4 or protamine). Interestingly, ternary complexes formed by pDNA, Lipofectamine and LD4 presented even more efficient pDNA delivery. In this case, we observed that in the presence of Lipofectamine™, complexes formed at 1:100 pDNA:protein molar ratio were more efficient than those formed at 1:8000. One possible explanation is that addition of Lipofectamine™ to the already compact complex formed by pDNA:LD4 (1:100) lead to the formation of more stable and even smaller complexes of approximately 100 nm, as can be seen in Fig. 5.

It is interesting to note that the addition of protamine to the ternary complex (1:8000:8000 pDNA:LD4:protamine), resulting in the formation of quaternary complexes, restored the transfection efficiency, indicating that synergic effects between the lipid and proteins are responsible for the increase in transfection efficiency. The increase in transfection efficiency promoted by protamine in multicomponent complexes have already been reported and was credited to its nuclear localization signal [35,37]. Despite this may also be the case of LD4, the observed increase in pDNA delivery of complexes containing LD4 at a low molar ratio (1:100) can also be explained by changes in complex stability, size, and the ability to overcome different barriers to the intracellular trafficking, including the recruitment of dynein motors. Synergic effects resulted from the combination of proteins and the cationic polymer PEI were also observed (Fig. 7B). Therefore, these multicomponent complexes may combine the high capacity of pDNA internalization of the cationic lipids or polymers with the enhanced capacity of transport through the cytoplasm and nuclear entrance of the protein vectors.

3.6. Cytoskeleton and endossome/lysosome involvement in the transfection efficiency of pDNA:LD4 complexes

Our expectation on the study of LD4 protein for pDNA delivery is set on the possibility that this protein could mediate pDNA trafficking throughout the cytoplasm *via* dynein retrograde transport following escape from endosomes. The insertion of a DNA binding domain at the protein N-terminus was decided based on the structural data of the LC8 protein, since interaction with the dynein motors occurs *via* C-terminus and dimer interface [38]. Since the dynein motor complex relies on the microtubule network to mediate the cellular transport, the use of microtubule depolymerizing agents, such as nocodazole, would abort the active transport resulting in the decrease of transfection efficiency.

Therefore, to evaluate the role of microtubules on pDNA:LD4 complexes (1:8000 pDNA:protein molar ratio) mediated gene transfer into HeLa cells, nocodazole was used. By using this drug, we observed a 49% decrease in the transfection efficiency (Fig. 8). Similarly, cytochalasin D was used to evaluate the effect of actin filaments disruption on transfection efficiency (Fig. 8). The disruption of the actin filaments lead to a decrease in transfection efficiency of 99%. The results indicate that pDNA:LD4 complexes strongly rely on the cells cytoskeleton for intracellular trafficking and pDNA delivery. However, the decrease in transfection efficiency caused by the disruption of the cytoskeleton has already been described in the literature using pDNA:Lipofectamine™ and pDNA:PEI (polyethyleneimine) complexes [39,40]. Despite microtubules tend to facilitate intracellular trafficking of vectors *via* active retrograde transport of the vesicles formed after endocytosis, they can also contribute to their degradation since most of the vectors remain entrapped inside late endosomes and lysosomes and are finally destroyed in these vesicles [41,42]. On the other hand, the observed decrease in transfection efficiency when cells were pre-treated with cytochalasin D can be credited to the role attributed to actin filaments in the early steps of complex entry in the cell [40] as they are important to receptor-mediated endocytosis and might be involved in other pathways of internalization [43]. Disruption of actin filaments tends to decrease the internalization of complexes and hence lower transfection efficiency.

In order to further investigate the endosomal entrapment, which stands as a limiting step for gene delivery efficiency [44] of the pDNA:LD4 complexes, we performed transfections of HeLa cells treated with the lysosomotropic agent chloroquine (Fig. 8). Cloroquine is a weak base that accumulates in acidic organelles such as late endosomes and lysosomes, raising the luminal pH of the organelles and avoiding enzymatic degradation of non-viral vectors [45]. This drug is frequently used to investigate the effect of the endosomal/lysosomal entrapment as a barrier to gene delivery, since its action causes a

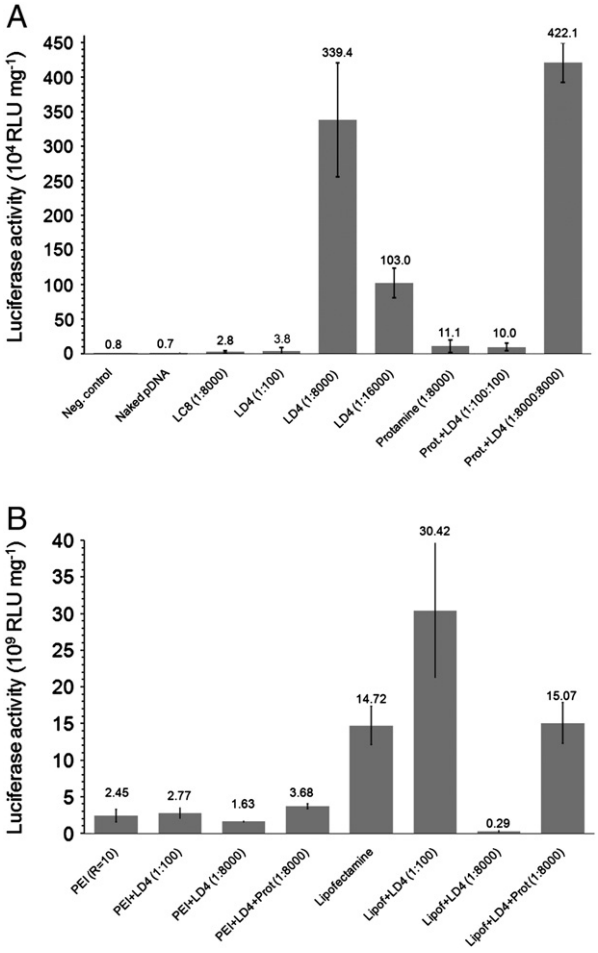

Fig. 7. A: Gene transfer to HeLa cells mediated by pDNA:LC8 and pDNA:LD4 complexes. Transfection efficiency was assessed by measuring the activity of the luciferase reporter gene. B: Comparison of the transfection efficiency of the LD4 fusion protein with the traditional delivery vectors PEI and Lipofectamine™. The combination of proteins (LD4 and protamine) with Lipofectamine™, resulting in ternary vectors, was also evaluated. Error bars indicate standard deviation between triplicates.

rise in intraendosomal osmolarity and its eventual lysis [46,47]. In our case, pre-treatment of HeLa cells with chloroquine (100 μM) enhanced the LD4 mediated transfection efficiency by 383%. Considering this data, escape from endosomes and lysosomes seems critical for the efficiency of LD4 mediated gene delivery and also for the understanding of the mechanisms of the intracellular trafficking of these pDNA:protein complexes. Beside this, we should also consider that an early release of pDNA:LD4 complexes in the cytosol promoted by chloroquine has another positive effect, since the complex may still rely on the retrograde transport to get closer to the cell nucleus *via* direct interaction between LD4 and dynein. In fact, we performed transfections using pDNA:protamine complexes in the presence of chloroquine and we found that the drug promoted an increase of 11-fold in Luciferase expression (Supplementary Data). Taking this result into account, LD4 seems to be more efficient in endosomal/lysosomal escape than protamine.

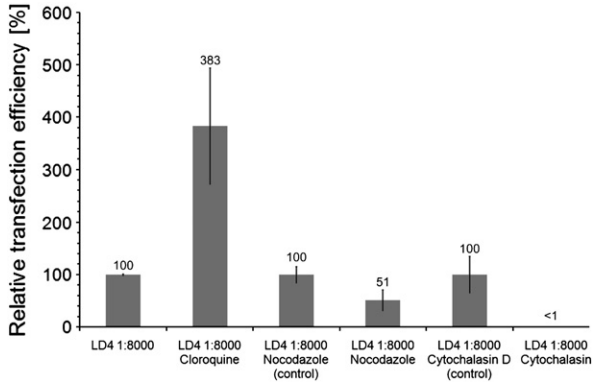

Fig. 8. Involvement of microtubules and endosomes/lysosomes on transfection efficiency of HeLa cells using LD4:pDNA complexes. The involvement of microtubules and actin were studied using the drugs nocodazole and cytochalasin D, respectively. The lysosomotropic agent chloroquine was used to investigate the effect of the endosomal/lysosomal entrapment as a barrier to gene delivery. Experiments were performed in triplicate as described in the Materials and methods section. Error bars indicate standard deviation between triplicates.

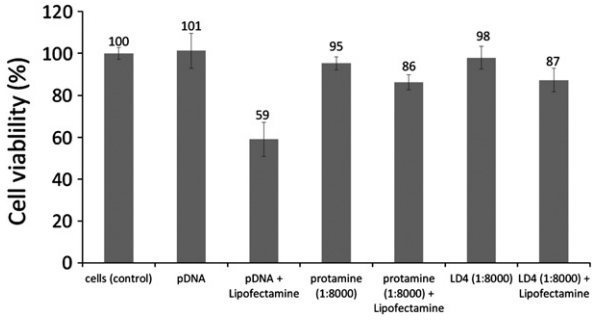

Fig. 9. Evaluation of the cytotoxicity of the different delivery vectors for HeLa cells performed using WST-1 reagent (Roche Applied Science). We assayed the cell viability after transfection with complexes formed by pDNA with lipofectamine, protamine and LD4 according to the procedure described in the Materials and methods section. Error bars indicate standard deviation between six replicates.

Finally, since both, pDNA:LD4 and pDNA:protamine, complexes used in this study have similar physical-chemical characteristics (size, charge ratio, nature, etc.), we believe that the differences found in transfection efficiency between LD4 and protamine mediated transfection (30-fold) may also be related to the natural ability of the LD4 to interact with the dynein motor and facilitate the intracellular trafficking. A complete study of the differences in intracellular trafficking of the different complexes studied here is still in progress by our research group. However, due to the complex nature of the vectors and the diversity of cellular entry pathways and intracellular trafficking, this is a very challenging task.

3.7. Plasmid DNA:LD4 complexes presented reduced cytotoxicity when compared to pDNA:Lipofectamine™ complexes

Cytotoxicity of the delivery vectors used in the present work was evaluated using the Cell Proliferation Reagent WST-1 (Roche Applied Science, USA) and cultivated HeLa cells. As expected, protein vectors proved to be far less toxic (98% and 95% cell viability for LD4 and protamine, respectively) than Lipofectamine™ (59% cell viability) (Fig. 9). Interestingly, the combination of LD4 and Lipofectamine™ lead to a reduced cell mortality comparing to the complex formed by cationic lipid and pDNA. So far, it is not clear the mechanisms behind the reduction of toxicity caused by the presence of the proteins in the ternary complexes. A possible explanation could be the reduction of the cationic lipid content in these complexes caused by competition with the proteins for the negatively charged plasmid backbone. Anyway, an important attribute of a gene delivery vehicle is the low toxicity, opening the possibility for a secure *in vivo* utilization, and the results indicate that pDNA:LD4 is a promising vector.

4. Conclusion

We presented here an innovative approach for the non-viral delivery of plasmid DNA. By combining the recombinant dynein light chain LC8 with a synthetic N-terminal DNA binding domain we were able to

construct a modular fusion protein specifically designed for gene delivery. The modified LC8, named LD4, was able to: i) interact and condense pDNA *in vitro* forming positively charged complexes and ii) to interact *in vitro* with dynein intermediate chain, confirming its functionality. Despite still far from being an optimized vector like the commercial lipids Lipofectamine™, LD4 proved to be 30-fold more efficient in transfection than protamine and 485-fold more efficient than naked DNA – this one the delivery method used in most of the non-viral clinical trials conducted so far. Transfection and cytotoxity assays also indicated that LD4 can be associated to cationic lipids to generate even more efficient delivery vectors for *in vitro* applications. Pre-treatment of the transfected HeLa cells with different drugs showed a major involvement of the cell's cytoskeleton in the intracellular trafficking, indicating the involvement of the dynein molecular motor in the transport of the pDNA:LD4 complexes. Despite the transfection results found using the LD4 vector are promising, the results also indicate the possibility of different forms of vector optimization, particularly particle charge and the ability to escape from endosomes/lysosomes. Finally, we believe that the work presented here add new information on the development of recombinant modular proteins specifically designed for gene delivery. By taking advantage of strategies used by virus to infect mammalian cells these vectors may, in the near future, increase the efficiency of non viral vectors and provide new tools for DNA vaccination and gene therapy studies.

Supplementary materials related to this article can be found online at doi:10.1016/j.jconrel.2012.01.011.

Acknowledgements

The authors gratefully acknowledge the financial support of the Fundação de Amparo à Pesquisa do Estado de São Paulo – FAPESP (São Paulo, Brazil). We also thank the Laboratório de Espectroscopia e Calorimetria (LEC), Laboratório Nacional de Biociências – LNBio (Campinas, Brazil), for the support on the circular dichroism studies and Professor Maricilda Palandi de Mello, CBMEG, UNICAMP (Campinas, Brazil), for the support on the HeLa cells culture. Finally, the authors thank Professor Ricardo Aparício, IQ, UNICAMP, for the help with the preliminary studies of SAXS and Professor Lucimara Gaziola de la Torre, FEQ, UNICAMP, for the help with potential zeta and particle size measurements.

References

[1] A. Arís, A. Villaverde, Modular protein engineering for non-viral gene therapy, Trends Biotechnol. 22 (7) (2004) 371–377.
[2] P. Saccardo, A. Villaverde, N. González-Montalbán, Peptide-mediated DNA condensation for non-viral gene therapy, Biotechnol. Adv. 27 (4) (2009) 432–438.
[3] M.L. Edelstein, M.R. Abedi, J. Wixon, Gene therapy clinical trials worldwide to 2007 – an update, J. Gene Med. 9 (10) (2007) 833–842.
[4] C. Liu, W. Yu, Z. Chen, J. Zhang, N. Zhang, Enhanced gene transfection efficiency in CD13-positive vascular endothelial cells with targeted poly(lactic acid)–poly(-ethylene glycol) nanoparticles through caveolae-mediated endocytosis, J. Control. Release 151 (2) (2011) 162–175.
[5] S. Höbel, A. Loos, D. Appelhans, S. Schwarz, J. Seidel, B. Voit, A. Aigner, Maltose- and maltotriose-modified, hyperbranched poly(ethylene imine)s (OM-PEIs): physicochemical and biological properties of DNA and siRNA complexes, J. Control. Release 149 (2) (2011) 146–158.
[6] C. He, Y. Tabata, J. Gao, Non-viral gene delivery carrier and its three-dimensional transfection system, Int. J. Pharm. 386 (1–2) (2010) 232–242.
[7] N. Ferrer-Miralles, E. Vázquez, A. Villaverde, Membrane-active peptides for non-viral gene therapy: making the safest easier, Trends Biotechnol. 26 (5) (2008) 267–275.
[8] J.M. Bergen, S.H. Pun, Evaluation of an LC8-binding peptide for the attachment of artificial cargo to dynein, Mol. Pharm. 4 (1) (2007) 119–128.
[9] M.A. Maslov, T.O. Kabilova, I.A. Petukhov, N.G. Morozova, G.A. Serebrennikova, V.V. Vlassov, M.A. Zenkova, Novel cholesterol spermine conjugates provide efficient cellular delivery of plasmid DNA and small interfering RNA, J. Control. Release (in press), doi:10.1016/j.jconrel.2011.11.023.
[10] T. Iida, T. Mori, Y. Katayama, T. Nidome, Overall interaction of cytosolic proteins with the PEI/DNA complex, J. Control. Release 118 (3) (2007) 364–369.
[11] M.E. Dowty, P. Williams, G. Zhang, J.E. Hagstrom, J.A. Wolff, Plasmid DNA entry into postmitotic nuclei of primary rat myotubes, Proc. Natl. Acad. Sci. U. S. A. 92 (1995) 4572–4576.
[12] G.L. Lukacs, P. Haggie, O. Seksek, D. Lechardeur, N. Freedman, A.S. Verkman, Size dependent DNA mobility in cytoplasm and nucleus, J. Biol. Chem. 275 (2000) 1625–1629.
[13] E. Mastrobattista, M.A. van der Aa, W.E. Hennink, D.J. Crommelin, Artificial viruses: a nanotechnological approach to gene delivery, Nat. Rev. Drug Discov. 5 (2) (2006) 115–121.
[14] T. Tzfira, On tracks and locomotives: the long route of DNA to the nucleus, Trends Microbiol. 14 (2) (2006) 61–63.
[15] G.W. Moseley, D.L. Leyton, D.J. Glover, R.P. Filmer, D.A. Jans, Enhancement of protein transduction-mediated nuclear delivery by interaction with dynein/microtubules, J. Biotechnol. 145 (3) (2010) 222–225.
[16] A.P. Carter, C. Cho, L. Jin, R.D. Vale, Crystal structure of the dynein motor domain, Science 331 (2011) 1159–1165.
[17] E.L. Holzbaur, R.B. Vallee, DYNEINS: molecular structure and cellular function, Annu. Rev. Cell Biol. 10 (1994) 339–372.
[18] R.B. Vallee, M.P. Sheetz, Targeting of motor proteins, Science 271 (1996) 1539–1544.
[19] K. Döhner, C.H. Nagel, B. Sodeik, Viral stop-and-go along microtubules: taking a ride with dynein and kinesins, Trends Microbiol. 13 (7) (2005) 320–327.
[20] G. Benison, P.A. Karplus, E. Barbar, The interplay of ligand binding and quaternary structure in the diverse interactions of dynein light chain LC8, J. Mol. Biol. 384 (4) (2008) 954–966.
[21] K.W. Lo, H.M. Kan, L.N. Chan, W.G. Xu, K.P. Wang, Z. Wu, M. Sheng, M. Zhang, The 8-kDa dynein light chain binds to p53-binding protein 1 and mediates DNA damage-induced p53 nuclear accumulation, J. Biol. Chem. 280 (2005) 8172–8179.
[22] S.R. Jaffrey, S.H. Snyder, PIN: an associated protein inhibitor of neuronal nitric oxide synthase, Science 274 (1996) 774–777.
[23] H. Puthalakath, D.C. Huang, L.A. O'Reilly, S.M. King, A. Strasser, The proapoptotic activity of the Bcl-2 family member Bim is regulated by interaction with the dynein motor complex, Mol. Cell 3 (3) (1999) 287–296.
[24] H. Puthalakath, A. Villunger, L.A. O'Reilly, J.G. Beaumont, L. Coultas, R.E. Cheney, D.C. Huang, A. Strasser, Bmf: a proapoptotic BH3-only protein regulated by interaction with the myosin V actin motor complex, activated by anoikis, Science 293 (5536) (2001) 1829–1832.
[25] F. Schnorrer, K. Bohmann, C. Nusslein-Volhard, The molecular motor dynein is involved in targeting swallow and bicoid RNA to the anterior pole of *Drosophila* oocytes, Nat. Cell Biol. 2 (2000) 185–190.
[26] K.W. Lo, S. Naisbitt, J.S. Fan, M. Sheng, M. Zhang, The 8-kDa dynein light chain binds to its targets via a conserved (K/R)XTQT motif, J. Biol. Chem. 276 (2001) 14059–14066.
[27] A.R. Azzoni, S.C. Ribeiro, G.A. Monteiro, D.M. Prazeres, The impact of polyadenylation signals on plasmid nuclease-resistance and transgene expression, J. Gene Med. 9 (5) (2007) 392–402.
[28] S.S. Freitas, A.R. Azzoni, J.L. Santos, G.A. Monteiro, D.M.F. Prazeres, On the stability of plasmid DNA vectors during cell culture and purification, Mol. Biotechnol. 36 (2007) 151–158.
[29] B.F. Caninie, Y. Wang, A. Hatefi, Evaluation of the effect of vector architecture on DNA condensation and gene transfer efficiency, J. Control. Release 129 (2008) 117–123.
[30] E. Barbar, B. Kleinman, D. Imhoff, M. Li, T.S. Hays, M. Hare, Dimerization and folding of LC8, a highly conserved light chain of cytoplasmic dynein, Biochemistry 40 (6) (2001) 1596–1605.
[31] J. Hall, P.A. Karplus, E. Barbar, Multivalency in the assembly of intrinsically disordered Dynein intermediate chain, J. Biol. Chem. 284 (48) (2009) 33115–33121.
[32] S. Xiang, et al., Uptake mechanisms of non-viral gene delivery, J. Control. Release (2011), doi:10.1016/j.jconrel.2011.09.093.
[33] M. Ikonen, L. Murtomäki, K. Kontturi, Controlled complexation of plasmid DNA with cationic polymers: effect of surfactant on the complexation and stability of the complexes, Colloids Surf., B 66 (1) (2008) 77–83.
[34] R. Balhorn, M. Cosman, K. Thornton, V.V. Krishnan, M. Corzett, G. Bench, C. Kramer, J.I.V. Lee, N.V. Hud, M. Allen, M. Prieto, W. Meyer-Ilse, J.T. Brown, J. Kirz, X. Zhang, E.M. Bradbury, G. Maki, R.E. Braun, W. Breed, Protamine-mediated condensation of DNA in mammalian sperm, in: C. Gagnon (Ed.), The male gamete: from basic knowledge to clinical applications, 1999, pp. 55–70.
[35] J. Chen, Z. Yu, H. Chen, J. Gao, W. Liang, Transfection efficiency and intracellular fate of polycation liposomes combined with protamine, Biomaterials 32 (5) (2011) 1412–1418.
[36] Y.J. Park, J.F. Liang, K.S. Ko, S.W. Kim, V.C. Yang, Low molecular weight protamine as an efficient and nontoxic gene carrier: in vitro study, J. Gene Med. 5 (8) (2003) 700–711.
[37] A. Noguchi, N. Hirashima, M. Nakanishi, Cationic cholesterol promotes gene transfection using the nuclear localization signal in protamine, Pharm. Res. 19 (7) (2002) 933–938.
[38] G. Benison, P.A. Karplus, E. Barbar, Structure and dynamics of LC8 complexes with KXTQT-motif peptides: swallow and dynein intermediate chain compete for a common site, J. Mol. Biol. 371 (2) (2007) 457–468.
[39] V. Ondřej, E. Lukášová, M. Falk, S. Kozubek, The role of actin and microtubule networks in plasmid DNA intracellular trafficking, Acta Biochim. Pol. 54 (3) (2007) 657–663.
[40] S. Grosse, Y. Aron, G. Thévenot, M. Monsigny, I. Fajac, Cytoskeletal involvement in the cellular trafficking of plasmid/PEI derivatives complexes, J. Control. Release 122 (2007) 111–117.
[41] S. Hasegawa, N. Hirashima, M. Nakanishi, Microtubule involvement in the intracellular dynamics for gene transfection mediated by cationic liposomes, Gene Ther. 8 (2001) 1669–1673.
[42] J. Suh, D. Wirtz, J. Hanes, Efficient active transport of gene nanocarriers to the cell nucleus, Proc. Natl. Acad. Sci. U. S. A. 100 (2003) 3878–3882.

[43] G. Apodaca, Endocytic traffic in polarized epithelial cells: role of the actin and microtubule cytoskeleton, Traffic 2 (2001) 149–159.
[44] A.K. Varkouhi, M. Scholte, G. Storm, H.J. Haisma, Endosomal escape pathways for delivery of biologicals, J. Control. Release 151 (3) (2011) 220–228.
[45] J. Pelisek, L. Gaedtke, J. DeRouchey, G.F. Walker, S. Nikol, E. Wagner, Optimized lipopolyplex formulations for gene transfer to human colon carcinoma cells under in vitro conditions, J. Gene Med. 8 (2006) 186–197.
[46] J.P. Behr, The proton sponge: a trick to enter cells the viruses did not exploit, Chimica 51 (1997) 34–36.
[47] L. Benimetskaya, N. Guzzo-Pernell, S.-T. Liu, J.C.H. Lai, P. Miller, C.A. Stein, Protamine-fragment peptides fused to an SV40 nuclear localization signal deliver oligonucleotides that produce antisense effects in prostate and bladder carcinoma cells, Bioconjug. Chem. 13 (2002) 177–187.

Journal of Biotechnology 173 (2014) 10–18

Contents lists available at ScienceDirect

Journal of Biotechnology

journal homepage: www.elsevier.com/locate/jbiotec

Development of a non-viral gene delivery vector based on the dynein light chain Rp3 and the TAT peptide

M.T.P. Favaro[a], M.A.S. de Toledo[a], R.F. Alves[b], C.A. Santos[a], L.L. Beloti[a], R. Janissen[c], L.G. de la Torre[d], A.P. Souza[a], A.R. Azzoni[b,*]

[a] Laboratório de Análise Genética e Molecular, Centro de Biologia Molecular e Engenharia Genética, Universidade Estadual de Campinas, Campinas, SP, Brazil
[b] Departamento de Engenharia Química, Escola Politécnica, Universidade de São Paulo, São Paulo, SP, Brazil
[c] Instituto de Física Aplicada "Gleb Wataghin", Universidade Estadual de Campinas, Campinas, SP, Brazil
[d] Faculdade de Engenharia Química, Universidade Estadual de Campinas, Campinas, SP, Brazil

ARTICLE INFO

Article history:
Received 16 October 2013
Received in revised form
20 December 2013
Accepted 2 January 2014
Available online 11 January 2014

Keywords:
Gene delivery
Non-viral protein vectors
Dynein light chain Rp3
TAT

ABSTRACT

Gene therapy and DNA vaccination trials are limited by the lack of gene delivery vectors that combine efficiency and safety. Hence, the development of modular recombinant proteins able to mimic mechanisms used by viruses for intracellular trafficking and nuclear delivery is an important strategy. We designed a modular protein (named T-Rp3) composed of the recombinant human dynein light chain Rp3 fused to an N-terminal DNA-binding domain and a C-terminal membrane active peptide, TAT. The T-Rp3 protein was successfully expressed in *Escherichia coli* and interacted with the dynein intermediate chain *in vitro*. It was also proven to efficiently interact and condense plasmid DNA, forming a stable, small (~100 nm) and positively charged (+28.6 mV) complex. Transfection of HeLa cells using T-Rp3 revealed that the vector is highly dependent on microtubule polarization, being 400 times more efficient than protamine, and only 13 times less efficient than Lipofectamine 2000™, but with a lower cytotoxicity. Confocal laser scanning microcopy studies revealed perinuclear accumulation of the vector, most likely as a result of transport *via* microtubules. This study contributes to the development of more efficient and less cytotoxic proteins for non-viral gene delivery.

1. Introduction

Gene therapy can be defined as the introduction of nucleic acids into cells with the goal of altering gene expression to prevent, halt or reverse a pathological process (Kay, 2011). Despite the great potential of these new therapies, gene therapy still faces major challenges because DNA requires a vector to protect and to transport it into the cell. An ideal vector should be safe, efficient and stable. However, finding such a vector remains a major challenge (Ganta et al., 2008; Ruponen et al., 2009). Viral vectors, biological carriers that have naturally evolved to transfer genetic materials into host cells (Lv et al., 2006), are efficient, although they are associated with several adverse effects ranging from inflammation to death, raising doubts about their safety (Edelstein et al., 2007; Vázquez et al., 2008). Non-viral vectors are less efficient but are considered to be safer, are cheaper to produce and have no limitations on the size of the DNA sequence delivered (Kay, 2011).

DNA delivery systems must overcome multiple extra- and intracellular barriers before reaching the nucleus. These barriers include binding to the cell surface, cell entry/endocytosis, endosomal escape, evasion of cytosolic nucleases and nuclear entry (Azzoni et al., 2007; Medina-Kauwe et al., 2005; Ruponen et al., 2009). One important obstacle that is often neglected in strategies that mimic viral trafficking is transport throughout the cytoplasm. Plasmid DNA cannot depend solely on diffusion during trafficking to the nucleus. Microinjection studies have demonstrated that naked pDNA larger than 2000 bp diffuses poorly if at all in the cytoplasm (Douglas, 2004; Lukacs et al., 2000; Suh et al., 2003). Additionally, free pDNA in the cytosol is rapidly degraded by endonucleases (Mastrobattista et al., 2006). Therefore, it has been suggested that dyneins may serve to improve the transport of pDNA toward the minus-end of microtubules (MT), which are usually located close to the cell nucleus (Döhner et al., 2005; Mesika et al., 2005; Moseley et al., 2010; Tzfira, 2006). Dynein is a multi-subunit protein complex formed by two dynein heavy chains (HC; ~530 kDa, responsible for ATP hydrolysis and binding to microtubules), two dynein intermediate chains (IC; ~74 kDa),

* Corresponding author at: Departamento de Engenharia Química, Escola Politécnica, Universidade de São Paulo, Av. Prof. Luciano Gualberto, Trav. 3, Nº 380, CEP 05508-900, São Paulo, SP, Brazil. Tel.: +55 11 30912234; fax: +55 11 30912284.
E-mail addresses: adriano.azzoni@poli.usp.br, adrianoazzoni@hotmail.com (A.R. Azzoni).

0168-1656/$ – see front matter © 2014 Elsevier B.V. All rights reserved.
http://dx.doi.org/10.1016/j.jbiotec.2014.01.001

several dynein light intermediate chains (LIC; ~52–61 kDa) and a number of dynein light chains (LC; ~10–25 kDa). The dynein light chains are from the LC8, TcTex/Rp3 and LC7/roadblock families and are responsible for cargo binding and the regulation of motor activity (Döhner et al., 2005; Holzbaur and Vallee, 1994).

Many viruses exploit microtubules *via* dynein motors to translocate to the nuclear periphery. For example, the herpes simplex virus type 1 binds to the dynein light chains Rp3 and TcTex1 to reach the nucleus (Dodding and Way, 2011; Douglas, 2004; Medina-Kauwe et al., 2005). The relevance of the microtubule network to the transport of pDNA complexes has been demonstrated (Suh et al., 2003), and the protein p53 also exploits this machinery to accumulate in the nucleus (Lo, 2004). Recently, Moseley et al. (2010) demonstrated that dynein light chain association sequences enhance the nuclear accumulation of exogenous proteins by exploring the MT network.

Our group recently demonstrated that the dynein light chain LC8 can be modified by inserting a synthetic DNA-binding motif while still maintaining the ability to interact *in vitro* with the dynein intermediate chain (Ferrer-Miralles et al., 2008; Toledo et al., 2012), forming positive particles that efficiently transfect HeLa cells *in vitro*. This process is dependent on MT transport and is minimally cytotoxic. We have also characterized the human dynein light chain Rp3 and shown that the simple addition of a DNA binding sequence transforms this dynein light chain into a promising gene delivery vector (Toledo et al., 2013). The human Rp3 has a molecular mass of approximately 13 kDa and is a member of the Tctex dynein light chain family. It exists in homodimeric and heterodimeric forms and is associated with Tctex1, although the heterodimer form is unable to bind to the dynein intermediate chain (King, 2000).

Here, recombinant Rp3 was fused to a N-terminal DNA binding domain and to the C-terminal TAT sequence, a cell penetrating peptide (CPP) (Azzoni et al., 2007; Won et al., 2011), to form a novel protein named T-Rp3. Cell penetrating peptides are also known as protein transduction domains (PTDs) and are usually short peptides that are rich in basic amino acids (Said Hassane et al., 2009). These peptides originate from proteins that are naturally capable of crossing membranes and have been used to study the delivery of bioactive molecules, including nucleic acids (Yamano et al., 2011). The better-known CPP is represented by TAT, an arginine-rich peptide derived from HIV-1 trans-activator protein (Won et al., 2011). The mechanism of TAT entry into the cell is the subject of some debate, but entry has been shown to be concentration and cell type-dependent (Ferrer-Miralles et al., 2008; Gump and Dowdy, 2007; Moschos et al., 2007). TAT is also promising for gene delivery because it has an additional ability of entering the cell nucleus with much faster kinetics than nuclear import mediated by the nuclear localization signal (NLS) (Nitin et al., 2009). In resume, this work presents a step forward on the development of modular proteins for non-viral gene delivery based on dynein light chains. Besides the inclusion of a new domain on the Rp3 protein, the TAT cell penetrating peptide, we could better characterize and evaluate the pDNA–protein complexes, transfection efficiency and cellular uptake of the non-viral particles, adding new information to the development of non-viral gene delivery vectors based on modular proteins.

2. Materials and methods

2.1. Plasmid DNA vector

The plasmid DNA used in this study was previously described by Toledo et al. (2012). Named pVAX1-Luc, the plasmid was constructed by replacing the GFP-encoding sequence of the pVAX1-GFP plasmid (Azzoni et al., 2007) with the luciferase gene sequence obtained from the pGL3-Luc control vector (Promega). Purification of the pVAX1-Luc plasmid used in all transfection studies was performed as described by Freitas et al. (2007).

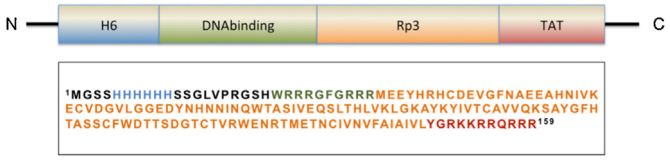

Fig. 1. The T-Rp3 recombinant protein. Illustrative distribution of functional modules in T-Rp3 and the amino acid sequence of the protein construct, which contains a histidine tail (H6 – in blue), the synthetic DNA-binding sequence (green), the Rp3 human dynein light chain (orange), and the TAT sequence (red). The residues resulting from the cloning process are shown in black. (For interpretation of the references to color in this figure legend, the reader is referred to the web version of the article.)

2.2. Recombinant protein expression and purification

The TAT DNA sequence was cloned into the pET28a expression vector (Merck). The TAT sequence was synthesized as two complementary single oligonucleotide strands containing the amino acid sequence YGRKKRRQRRR (Nitin et al., 2009) optimized for expression in *Escherichia coli*. The complementary sequences were annealed and phosphorylated prior to cloning in pET28a, which was previously digested with *Eco*RI and *Xho*I. The vectors were then transformed into *E. coli* strains.

The fusion protein DNA-binding domain WRRRGFGRRR (named DNAb4) was previously designed by Toledo et al. (2012) for peptide and protein domains with high DNA binding and condensing capacity. The DNAb4 domain was fused to the Rp3 sequence amplified from HeLa cell cDNA as described previously (Toledo et al., 2012). The Rp3 protein sequence containing the DNA-binding sequence was amplified and inserted in the pET28a plasmid encoding the TAT sequence described above using specific primers (forward: 5′-GATAATGCTAGCTGGCGTCGCCGTGGTTTTG-3′ and reverse: 5′-GCAAGCCTTAAGAAGAACAATAGCAATGGCAA-3′). The fragment was cloned into the pET28a vector (Merck) using the *Nhe*I and *Eco*RI restriction sites. The resulting fusion protein (DNAb4-Rp3-TAT) is named T-Rp3 (Fig. 1).

The recombinant T-Rp3 was expressed in *E. coli* BL21 (DE3). Briefly, cells were grown in 1 L of LB media at 37 °C with shaking at 300 rpm until an optical density of 0.8 AU was reached (measured at 600 nm). Protein expression was induced with 5.6 mM lactose for an additional 20 h at 28 °C and shaking at 200 rpm. After centrifugation, the cell pellet was resuspended in 50 mM Tris (pH 7.0), 1 M NaCl, 0.1 mM EDTA, 15 mM β-mercaptoethanol and 1 mM PMSF (phenylmethylsulfonyl fluoride). Cell lysis was achieved by sonication and the lysate was clarified by centrifugation (12,000 × *g* for 20 min). The T-Rp3 in the clarified lysate was purified by a single Ni-NTA affinity chromatography step and eluted using an imidazole gradient in suspension buffer. The protein was then dialyzed in 40 mM HEPES buffer (pH 7.3), a condition that favored protein stability.

2.3. In vitro interaction of T-Rp3 with the dynein intermediate chain

To assess the interaction of the recombinant T-Rp3 with the dynein complex, we expressed and purified the N-terminus (first 300 amino acids) of the human dynein intermediate chain DYNIC2, isoform C, according to the protocol described by Toledo et al. (2012). The purified protein was subsequently immobilized in CNBr-activated Sepharose resin (GE Healthcare) following the manufacturer's protocol. The resin was packed into a 1-mL gravity column (Bio-rad). The protein solution loaded onto the resin

was composed of an equimolar mixture of T-Rp3 and Lc8 in 40 mM HEPES buffer (pH 7.3). The Lc8 intermediate chain was produced as previously described (Toledo et al., 2012). The inclusion of Lc8 was based on the premise that the presence of one light chain enhances the affinity of a second light chain to the dynein intermediate chain (Makokha et al., 2002; Hall et al., 2009). The washing step was conducted using adsorption buffer and elution was performed with an increasing concentration of salt (0.1, 0.5 and 1.0 M NaCl). A final desorption step was performed at pH 3.0. The pH of the latter elution fractions was immediately raised using Tris buffer (pH 9.0). Finally, the protein profiles of the collected fractions were analyzed by SDS-PAGE.

2.4. Evaluation of pDNA–protein interaction by gel retardation assay

To evaluate the ability of T-Rp3 and protamine to interact and condense pDNA, we performed a gel retardation assay. Proteins were dialyzed in 40 mM HEPES (pH 7.3) and incubated with 1 μg of pVAX1-Luc vector (previously in PBS) at different pDNA:protein molar ratios (1:100, 1:200, 1:500, 1:1000, 1:4000 and 1:8000) in a final volume of 50 μL. Protamine sulfate powder was resuspended in PBS. The samples were incubated at room temperature for 1 h, followed by the addition of 50 μL of non-supplemented F-12 media and an additional incubation for 20 min. Samples were run on a 0.8% agarose gel and visualized by ethidium bromide staining.

2.5. Zeta potential and dynamic light scattering assays

Zeta potential measurements were performed to comparatively evaluate the surface charge of complexes formed by pDNA:T-Rp3 at different molar ratios. Complexes were formed as previously described for the gel retardation assay, but without adding F-12 media. Each sample was measured six times using the Malvern Zetasizer Nano ZS (Malvern). The average hydrodynamic diameter and size distribution (number-weighted) of the complexes were measured *via* the dynamic light scattering (DLS) as described by Toledo et al. (2012). The pDNA:T-Rp3 complexes were measured at a molar ratio of 1:8000. Complexes were formed with 1 μg of pDNA and the corresponding amount of protein in a final volume of 800 μL. Each sample was subjected to multiple readings in a 60-min period.

2.6. Culture and transfection of HeLa cells

HeLa cells were grown in a F-12 (Ham) nutrient mixture (Gibco) containing 10% (v/v) fetal bovine serum (growth medium, Gibco). The cells were cultured in 75 cm^2 culture flasks and incubated in a 5% CO_2 humidified environment at 37 °C. Following growth to confluence, cells were trypsinized and seeded in 24-well culture plates (5×10^4 cells per well). The cells were incubated for 48 h (to 70% confluence) and then transfected with pDNA:protein complexes formed as described previously for gel retardation assays, using the same molar ratios. When indicated, transfection was carried out using the Lipofectamine 2000™ reagent (Invitrogen) according to the manufacturer's instructions (1 μg pDNA plus 1.5 μL reagent in 100 μL of medium per well) or protamine sulfate (Sigma–Aldrich, Germany). All transfections were carried out in the presence of serum. The medium containing the transfection solution remained on the transfected cells for 6 h and was then replaced with fresh growth medium. Cells were collected 24 h post-transfection and luciferase activity was determined by utilizing the Luciferase Assay System (Promega) according to the manufacturer's instructions. Luminescence intensity was normalized against the protein concentration in each transfection sample, determined by the Micro BCA Protein Assay Kit (Thermo Scientific). We used Lipofectamine 2000™ as a control because it is regarded as an effective and fast-acting transfection agent. The transfection assays were performed as three independent replicates (experiments performed independently), except using protamine (eight independent replicates), T-Rp3 (twelve independent replicates) and Lipofectamine 2000™ (six independent replicates).

To evaluate the contribution of the microtubule network in the intracellular trafficking of the complexes, cells were pre-incubated for 2 h with nocodazole (25 μM) (Sigma–Aldrich) to disrupt the microtubules. The drug was dissolved in DMSO and an equal volume of drug-free DMSO (0.4%) was used as a control. Transfections were performed in the presence of chloroquine to evaluate the contribution of lysosomal degradation of pDNA:protein complexes. Cells were pre-incubated for 4 h with chloroquine (100 μM) (Sigma–Aldrich). For these assays, pre-treated cells were incubated in the presence of different complexes for 4 h, after which the medium was replaced with fresh growth medium. After 24 h, cells were collected, and the luciferase activity was measured as described above. The experiments were performed as three independent replicates and the results were normalized as percentages, and the value of luciferase expression (in RLU/mg) of the control was defined as 100%.

2.7. In vitro toxicity

Cytotoxicity of the delivery vectors was assessed using the Cell Proliferation Reagent WST-1 (Roche Applied Science) following the manufacturer's instructions. Briefly, HeLa cells were grown in 96-well plates to 70% confluence and then transfected as described above with pDNA:protamine (pDNA:protein molar ratio of 1:8000) or pDNA:T-Rp3 (pDNA:protein molar ratio of 1:8000) complexes with and without Lipofectamine 2000™; pDNA alone served as the control. The experiments were performed as six independent replicates. The complexes were prepared as previously described (item 2.5) using a final volume (20 μL) proportional to the 96 wells. The mass of pDNA used per well was 0.2 μg and all pDNA:protein molar rations were kept the same. Lipofection using Lipofectamine 2000™ was carried out using 0.2 μg pDNA plus 0.3 μL reagent in 20 μL of medium per well. The cells were exposed to the complexes for 6 h, when the medium was replaced. The plates were analyzed 24 h post-transfection. Analysis was done by adding 10 μL of WST-1 reagent to each well, followed by incubation for an additional hour. Absorbance was recorded at 440 nm in an ELISA reader.

2.8. Cellular uptake

Cellular uptake and trafficking of vectors were examined using a Zeiss LSM780-NLO laser scanning confocal microscope with a Plan-Apochromat 63× oil objective (NA 1.45). Plasmids pVAX1-LUC were covalently labeled with Cy3™ (Label IT, Mirus) and used for HeLa cell transfection as previously described. Cells were collected at different time points (6, 12 and 24 h post-transfection), rinsed with PBS, fixed (formaldehyde 3.7% in PBS for 5 min), permeabilized and blocked. For microtubule staining, cells were incubated with anti-α-tubulin overnight followed by incubation with Alexa Fluor™ 488-coupled secondary antibody (both from Molecular Probes-Invitrogen) for 2 h. After washing in PBS, cells were stained with 4,6-diamino-2-phenylindole (DAPI), washed again and kept in PBS. The 3D image measurements through the depth of the cell were reconstructed and deconvoluted using AutoQuantX2 (Media Cybernetics Inc., USA). All deconvoluted image stacks were further reconstructed by voxel-based volume and isosurface rendering using Imaris (Bitplane) to determine the localization of the vector particles within the cells.

2.9. Time-lapse microscopy

Time-lapse imaging assays were performed on live HeLa cells (phase) transfected with pDNA:T-Rp3 complexes (Cy3-labeled pDNA, in red). HeLa cells were seeded on a sterile 35-mm glass bottom dish (Hi-Q4 culture dish) and grown to 40% confluence. The medium was then replaced by a fresh medium containing the labeled complexes and the culture dish was placed into the live-imaging chamber of a Nikon BioStation IM-Q (Nikon). Multiple image capture points were selected and captured for 11 h using 20× magnification. Time-lapse microscopy was also performed in the presence of chloroquine.

2.10. Statistics

Statistical significance of the transfection results (transfection level, effect of drugs and cytotoxicity) was determined using the two-tailed Student's *t*-test, assuming unequal variances, at a significance level $p < 0.05$. The data were presented as the mean ± standard deviation. The number of independent experiments in each analysis is presented in Section 2. Analyses were performed using the Microsoft Excel Data Analysis ToolPack 2007 (Microsoft).

3. Results and discussion

3.1. T-Rp3 fusion protein expression in E. coli

During the design of a novel modular protein, special care should be taken to avoid steric hindrance of the functional domains or sequences. We have recently reported the cloning, purification and structural characterization of human Rp3 to determine its potential use as a gene carrier (Toledo et al., 2013). Here, the cloning of a new protein (T-Rp3) was performed with the insertion of a TAT sequence at the C-terminus of the Rp3 protein, in addition to the fusion of the histidine tail and the DNA-binding domain to the N-terminus (Fig. 1). This construction was chosen to prevent the blockage of domains involved in the interaction with the dynein motor complex, based on the available structural data for TcTex (Williams, 2005) and dynein complex formation data (Barbar et al., 2001). We also took into consideration a low-resolution structural model generated by SAXS for the recombinant Rp3 (Toledo et al., 2013). The short TAT sequence (11 amino acid residues) was fused to the C-terminus of the Rp3 protein to increase the probability of this membrane active sequence to be exposed following complex formation with pDNA.

3.2. T-Rp3 interaction in vitro with dynein intermediate chain

After the successful expression and purification of T-Rp3 (Supplementary data, Fig. 1S), we evaluated whether the recombinant protein retained the ability to interact with the dynein intermediate chain *in vitro*. Since C-terminal region of T-Rp3 contains TAT peptide and is probably involved in light chain dimerization and interaction with the dynein complex (Makokha et al., 2002), we analyzed the interaction of recombinant T-Rp3 with human dynein intermediate chain DYNIC2 (isoform C) *in vitro*. The results of the affinity chromatography assay indicated a strong interaction between T-Rp3 and the immobilized intermediate chain, as shown in the SDS-PAGE gel prepared with the fractions collected during the chromatography steps (Fig. 2A). The T-Rp3 could only be eluted from the column containing the immobilized intermediate chain under strongly acidic conditions (pH 3.0). Additionally, this interaction could not be disrupted by a salt gradient, which also pointed to a specific interaction between the recombinant light chains and the immobilized intermediate chain. As a control, we performed

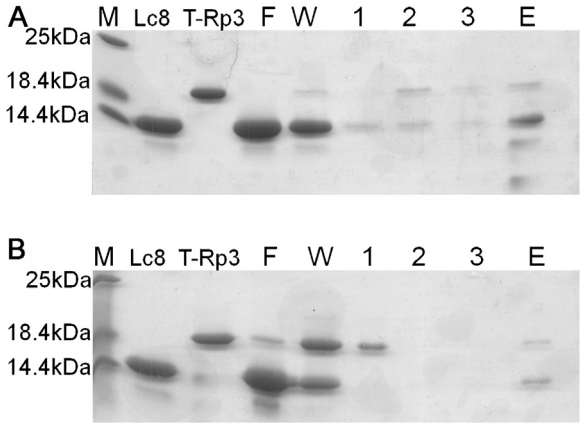

Fig. 2. T-Rp3 interacts with the dynein intermediate chain. The T-Rp3 interaction with the dynein intermediate chain was evaluated in the presence of Lc8 by affinity chromatography in immobilized intermediate chain Sepharose resin. The fractions collected were analyzed in a SDS-PAGE gel. The lanes labeled T-Rp3 and Lc8 represent the proteins alone, before preparation of the equimolar solution. We observed a much stronger interaction in the resin with the immobilized intermediate chain (A) than with the control resin (B). After flow-through (lane F) and washing (lane W), three additional washing steps were performed with an increasing salt gradient (lanes 1–3), and a final step using a pH 3.0 elution buffer (lane E).

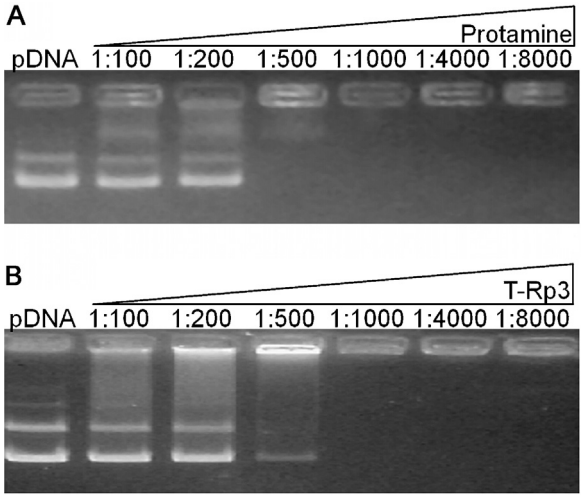

Fig. 3. T-Rp3 interacts with and condenses pDNA. The ability of protamine (A) and T-Rp3 (B) to interact with and to condense plasmid DNA was analyzed by gel retardation assays. Six pDNA:protein molar ratios were studied, as shown in the gel captions.

the chromatography using a resin without the intermediate chain (CNBr-activated Sepharose blocked with Tris) and observed only nonspecific interaction, with most of the T-Rp3 being eluted during the flow-through, washing and salt gradient steps (Fig. 2B). Taken together, these are strong indications that the recombinant T-Rp3 retains the ability to interact with the dynein intermediate chain *in vitro*.

3.3. T-Rp3 interaction with plasmid DNA

Gel retardation assays (Fig. 3) demonstrate that the interaction of T-Rp3 with pDNA is molar ratio dependent, with similar results to protamine, an arginine-rich protein important in spermatogenesis, responsible for inducing torus formation and DNA packaging (Brewer, 1999). This effect can be attributed to the addition of DNA-binding and TAT domains, as both are positively charged. In agreement with this observation, wild-type Rp3 (without DNA-binding or TAT) exhibits no significant capacity to interact with

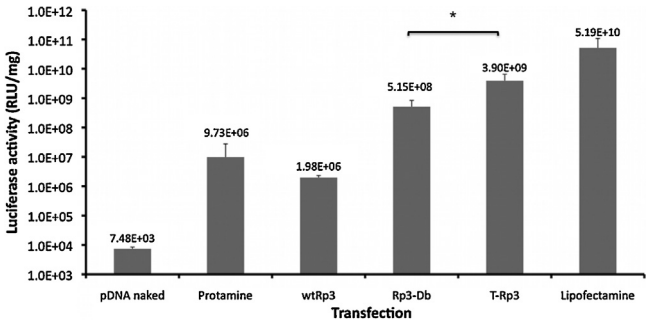

Fig. 4. Compared efficiency of T-Rp3. Transfection efficiency of HeLa cells comparing naked pDNA, protamine, wild-type Rp3 (Rp3), Rp3 containing the synthetic DNA-binding sequence (Rp3-Db), T-Rp3 (containing the DNA-binding and TAT sequences), and Lipofectamine 2000™. The molar ratio used for all pDNA:protein complexes was 1:8000. Transfection efficiency was assessed by measuring the activity of the luciferase reporter enzyme. Error bars indicate the standard deviation of replicates (See Section 2). The signal (*) indicates that the results are significantly different ($p < 0.05$) when compared between the pairs. The *y*-axis is presented using a $\log_{10}$ scale.

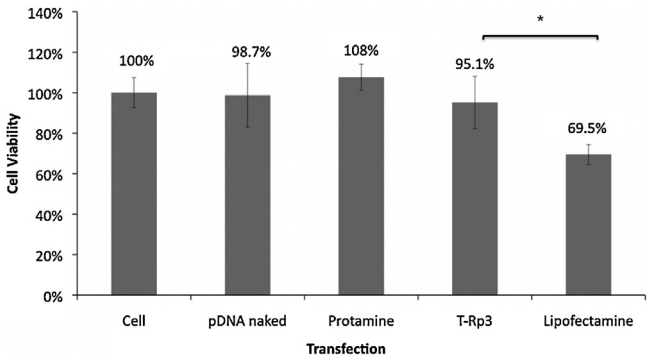

Fig. 5. Evaluation of the cytotoxicity of different delivery vectors for HeLa cells. The assays were performed using the WST-1 reagent (Roche Applied Science). We assayed cell viability following transfection with complexes formed by pDNA and Lipofectamine 2000™, protamine and T-Rp3 as previously described. Error bars indicate the standard deviation of six replicates performed independently. The signal (*) indicates that the results are significantly different ($p < 0.05$) when compared between the pairs.

pDNA, even at higher molar ratios (data not shown). Analysis of the zeta potential of the pDNA:T-Rp3 particles shows that it has a positive charge (+28.6 mV) at the 1:8000 molar ratio, while the pDNA:protamine net charge was +14.3 mV. Furthermore, dynamic light scattering assays indicate that at a molar ratio of 1:8000, the pDNA:T-Rp3 particles are smaller and more stable when compared to protamine under the same conditions. While pDNA:protamine particle size increased from 213 to 575 nm in 1 h, T-Rp3 formed smaller particles (77 nm) that did not increase much in size (95 nm) after the same period (Supplementary data, Fig. 2S).

3.4. Evaluation of T-Rp3 mediated gene delivery in cultured HeLa cells

The efficiency of pDNA delivery mediated by T-Rp3 in cultured HeLa cells was evaluated and compared to the efficiency of the wild-type Rp3 (wtRp3) and a T-Rp3 construct lacking the TAT sequence (Rp3-Db), as well as protamine. As observed in Fig. 4, wtRp3 presented a significant but limited efficiency to deliver pDNA. This can be explained by the low theoretical isoelectric point of wtRp3 (p*I* of 6.0), which results in a weak electrostatic interaction with pDNA, as verified by the gel retardation assay (data not shown). The insertion of the N-terminus synthetic DNA-binding (Rp3-Db) increased luciferase expression by 260 times. However, the addition of the TAT and DNA-binding sequences to Rp3 (T-Rp3) was associated with an approximately 2000-fold increase in luciferase expression. In fact, the transfection efficiencies of T-Rp3 and Rp3-Db were not much different as initially expected. However, although these two proteins have not been compared under every aspect, the addition of the TAT domain to Rp3-Db (T-Rp3) still increased the vector efficiency by 7.6-fold ($p < 0.05$). Moreover, T-Rp3 is more stable and allows easier manipulation during protein purification steps, probably as a result of the higher p*I* and reduced propensity to electrostatic aggregation (data not shown).

Compared to protamine, T-Rp3 presented a 400-fold increase in transgene expression, and a 13-fold increase was found in comparison to the previously reported LD4, the LC8 based recombinant protein (Toledo et al., 2012). The molar ratios used were chosen based on our previous experience (Toledo et al., 2012) and from preliminary studies comparing the transfection efficiency of protamine and T-Rp3 at different molar ratios (data not shown). The 1:8000 pDNA:protein molar ratio was found to be the best, similarly to our previous results with LD4 (Toledo et al., 2012). High molar ratios are necessary to form particles with high zeta potential values, which may contribute to a reduced propensity to aggregate and to promote high transfection efficiencies. Furthermore, in the case of T-Rp3, the increase in the number of TAT sequences on the surface of the cargos (complexes) may also increase their efficiency of escape from endosomes/lysosomes during intracellular trafficking (Erazo-Oliveras et al., 2012).

In addition, we compared the transfection efficiency of T-Rp3 to Lipofectamine 2000™, a cationic lipid that is highly efficient *in vitro*. The pDNA delivery mediated by Lipofectamine 2000™ resulted in a luciferase expression 13 times higher than that found for T-Rp3 (Fig. 4). Lipofectamine 2000™ is known to improve endosomal escape and delivery to the cytosol, including a fast nuclear translocation capability (Akita et al., 2004). For a better evaluation of the T-Rp3 efficiency, we performed transfections using the pVAX1-GFP plasmid, which differs from pVAX1-Luc by the presence of a *GFP* reporter gene instead of *luciferase* (Azzoni et al., 2007). Flow cytometry analysis of the HeLa cells transfected by the pDNA:T-Rp3 complexes resulted in a value of 14% of positive cells, while the value found for Lipofectamine 2000™ was 23%.

3.5. Evaluation of cytotoxicity

Transfection efficiency is not the only important characteristic of a non-viral vector designed for *in vivo* studies. Vectors should also be of low cytotoxicity and immunogenicity. An advantage of T-Rp3 is that most of its amino acid sequence is composed by the human dynein light chain Rp3, which is endogenously expressed in human cells (King, 2000). In a comparative study of efficiency and toxicity of four different protein transduction domains, the TAT sequence was found to be of low cytotoxicity to HeLa cells (Sugita et al., 2009). We also performed an evaluation of the *in vitro* toxicity of T-Rp3, protamine and Lipofectamine 2000™ by measuring the activity of mitochondrial dehydrogenase (Fig. 5). Protamine and T-Rp3 had a reduced toxic effect and, as expected, Lipofectamine 2000™ had the highest cytotoxicity for HeLa cells, with a decrease in cell viability of approximately 30%. The cytotoxic effects of cationic lipids and especially Lipofectamine 2000™ have been reported by others (Spagnou et al., 2004; Zhang et al., 2007).

3.6. Microtubule involvement and endosomal escape

As discussed above, among the desired features of pDNA:T-Rp3 particles have the ability to interact with the microtubule network for fast intracellular trafficking and an improved endosomal escape capability. To evaluate the dependence of these particles on the microtubules, we performed transfections in the presence of

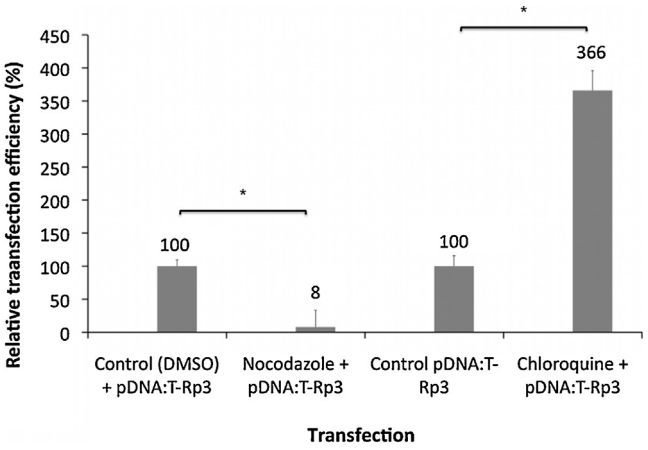

Fig. 6. Involvement of microtubules and endosomes in the transfection efficiency of HeLa cells using T-Rp3:pDNA complexes at a 1:8000 pDNA:T-Rp3 molar ratio. The involvement of microtubules was studied using nocodazole. Chloroquine was used to investigate the effect of the endosomal/lysosomal entrapment as a barrier to gene delivery. Error bars indicate the standard deviation of triplicate measurements performed independently. The signal (*) indicates that the results are significantly different ($p < 0.05$) when compared between the pairs.

nocodazole, a microtubule-depolymerizing agent that is expected to decrease the delivery efficiency of T-Rp3. In fact, in the presence of this drug, luciferase expression was reduced by 92%, suggesting that T-Rp3 is highly dependent on microtubules for pDNA delivery (Fig. 6). This is an interesting result and an indication that microtubules are involved in the transport of T-Rp3 complexes. For comparison, transfections performed with protamine and Lipofectamine 2000™ exhibited much smaller decrease in luciferase expression in the presence of nocodazole (56% and 41%, respectively). However, these results were not statistically significant at a significance level of $\alpha = 0.05$ (data not shown). Although this is not a proof of direct and specific interaction with dyneins, these results indicate that pDNA:T-Rp3 complexes strongly rely on active transport along microtubules to reach the nucleus.

Additionally, we assessed the level of entrapment of pDNA:T-Rp3 particles inside endosomes and lysosomes, which is another major limiting step in efficient gene delivery. Transfections were performed in the presence of chloroquine, a weak base that is often used to investigate endosomal entrapment. Chloroquine accumulates in acidic organelles such as late endosomes and lysosomes, raising the luminal pH of the organelles and preventing enzymatic degradation of non-viral vectors. Under the conditions tested, we observed that chloroquine promoted an approximately 4-fold increase in the reporter enzyme expression (Fig. 6). This finding indicates that endosomal entrapment remains an important limiting factor despite the presence of an N-terminal histidine tail and a C-terminal TAT sequence. Although it is reported that TAT-delivered cargos frequently remain trapped inside endocytic organelles (Brooks et al., 2005; Erazo-Oliveras et al., 2012), the presence of histidine residues (six in T-Rp3) tends to induce a proton sponge effect in such organelles, which increases their osmolarity, promotes swelling and, ultimately, lysis. For this reason, during the design of a gene vehicle, we should also take in consideration that an excessive increase in endo/lysosomal escape capability can result in higher cytotoxic effects due to vesicle disruptions and the release of pro-apoptotic and cytotoxic proteases.

3.7. Investigation of cellular uptake using confocal microscopy

Generally, the internalization of plasmid DNA particles mediated by TAT or arginine-rich peptides (such as the synthetic DNA-binding sequence in T-Rp3) occurs by endocytosis, mostly *via* the clathrin-dependent pathway, although a multiplicity of different entry pathways also tends to occur in parallel (Brooks et al., 2005). Here, we visualized the cellular uptake of pDNA:T-Rp3

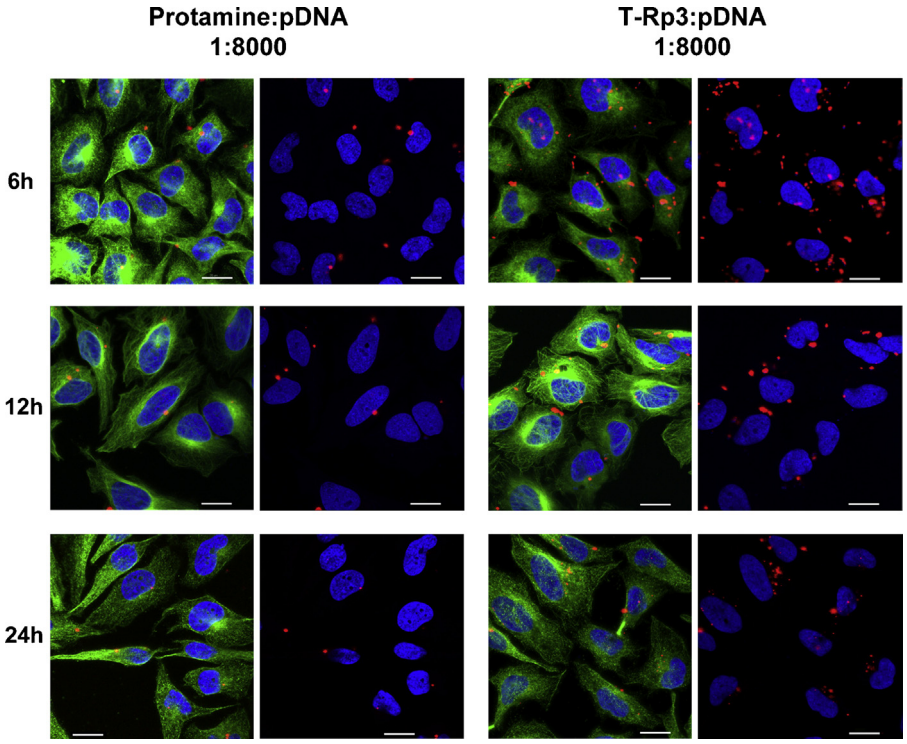

Fig. 7. Intracellular distribution of Cy3-labeled plasmid DNA in transfected HeLa cells. Transfections were mediated by protamine or T-Rp3 and images were collected at different time points by laser scanning confocal microscopy. Plasmid DNA can be seen in red (Cy3), microtubules are shown in green (Alexa Fluor 488), and the nuclei in blue (Dapi). Scale bars represent 20 μm. (For interpretation of the references to color in this figure legend, the reader is referred to the web version of the article.)

and pDNA:protamine complexes by HeLa cells at three different time points (6, 12 and 24 h post-transfection) (Fig. 7). The first difference observed was that, after washing and fixing, a higher amount of pDNA was internalized by cells transfected using T-Rp3, confirming the higher efficiency indicated by the luciferase expression results (Fig. 5). The pDNA distribution pattern, mainly in large and well-defined spots, is consistent with internalization by endocytosis and entrapment inside vesicles that tend to reduce in number overtime. This observation is also consistent with the results of the transfections performed in the presence of chloroquine (Fig. 6). However, despite the risk of artifacts due to fixation procedures, a difference in distribution pattern can be observed between the pDNA delivered by T-Rp3 and protamine. Compared to the protamine-mediated delivery, pDNA internalized by T-Rp3 is frequently observed not only inside large vesicles but also as small particles in the cytosol, indicating differences in the cellular uptake pathway and/or improved endosomal escape capability. This result is consistent with our data indicating that transfection efficiency mediated by protamine increases 10-fold in the presence of chloroquine (Toledo et al., 2012) in comparison with the 4-fold increase observed in T-Rp3 mediated transfections (Fig. 6).

At 6 h post-transfection, pDNA can be observed in the nucleus. This result was expected because a significant level of luciferase activity is detected at this time point (Supplementary data, Fig. 3S). Over time, pDNA red fluorescence is reduced, probably due to the degradation inside endosomal/lysosomal vesicles, as indicated by the presence of large red vesicles observed at 12 h post-transfection. Interestingly, differently from protamine, a significant amount of pDNA can be observed in the cells 24 h after T-Rp3 mediated transfection. Additionally, the vectors (Cy3-labeled pDNA, seen in red) are frequently concentrated at the perinuclear region of the cells, tending to co-localize with a dense concentration of microtubules (probably centrosomes), as can be observed in Figs. 8 and 4S. In contrast, protamine-mediated transfection frequently leads to cells containing only one or two large red spots, probably formed by pDNA trapped inside vesicles, and usually not co-localizing with dense microtubule concentrations (Fig. 7). The significant differences in cell uptake between T-Rp3 and protamine-mediated transfection were also captured by time-lapse live cell imaging (Videos 1 and 2, Supplementary data).

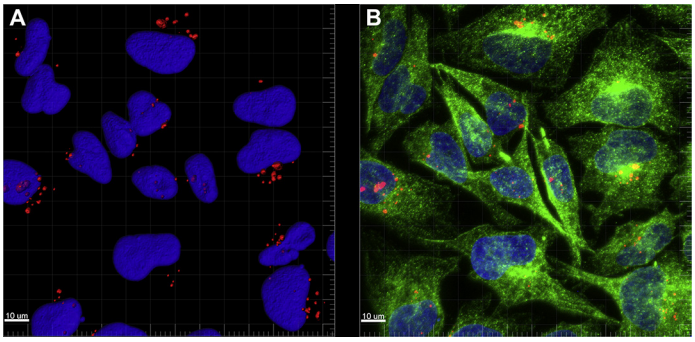

Fig. 8. Three dimensional distribution of Cy3-labeled pDNA (red) in HeLa cells transfected with pDNA:T-Rp3 complexes (A), indicating the presence of pDNA at the proximity of the nuclei (blue). Images were taken 24 h post-transfection using a laser scanning confocal microscope and were deconvoluted during post-processing. (B) Microtubules are stained in green (Alexa Fluor 488) and pDNA tends to co-localize with a dense concentration of microtubules. (For interpretation of the references to color in this figure legend, the reader is referred to the web version of the article.)

The images of intracellular trafficking of Lipofectamine 2000™-mediated transfections are not presented here, due to the distinct nature of this cationic lipid in comparison to protein vectors, and to the fact that it has been the subject of previous studies (Akita et al., 2004; Kamiya et al., 2002). Although cellular uptake of pDNA:Lipofectamine complexes occur mainly by endocytosis, escape from endosomal/lysosomal vesicles and nuclear translocation is faster and more efficient than peptide-mediated transfections, which is consistent with the high transfection efficiency of this lipid (Akita et al., 2004).

Time-lapse microscopy of the transfected cells in the presence of chloroquine indicated that perinuclear localization of the complex is fast (within less than 1 h), occurring during the period necessary for the setting of the live image equipment (Fig. 9). The pDNA:T-Rp3 complexes tended to accumulate in the perinuclear region of the cells even in the presence of chloroquine. This observation suggests

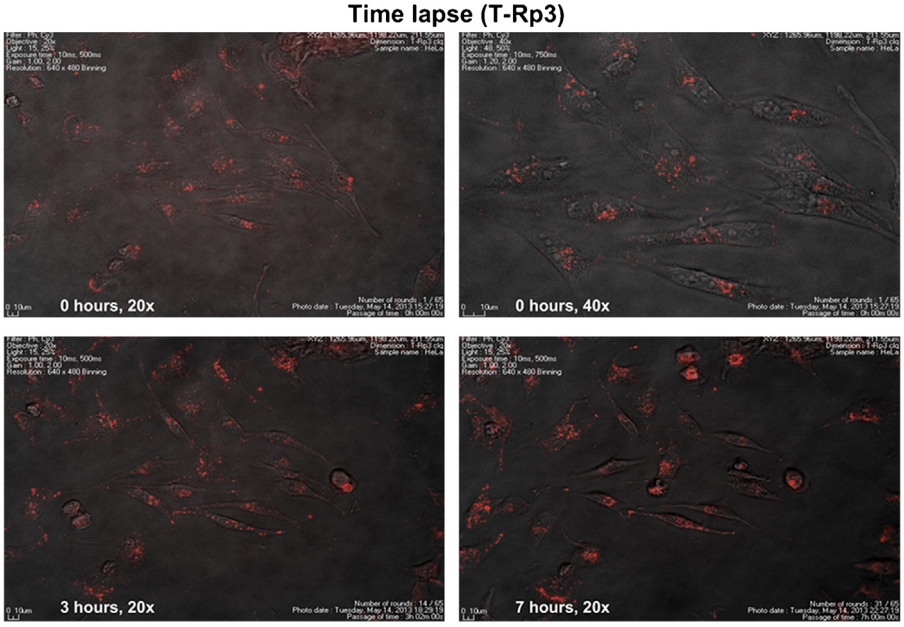

Fig. 9. Sequences of photographs taken from time-lapse imaging experiment at three different times after the transfection of HeLa cells (phase) with pDNA:T-Rp3 complexes (Cy3-labeled pDNA in red) and in the presence of chloroquine. The images taken at "0 h" (corresponding to approximately 1 h post-transfection, due to the time necessary to set the equipment) show a high level of complex internalization. The images also indicate that pDNA tends to accumulate at the proximity of the nuclei even in the presence of chloroquine. (For interpretation of the references to color in this figure legend, the reader is referred to the web version of the article.)

that active transport of the complexes occurs as a result of not only the movement of endocytic vesicles toward lysosomes but also the interaction of free pDNA:T-Rp3 complexes with microtubules.

4. Conclusion

We designed the recombinant protein T-Rp3 as a modular protein with the intention to mimic viral vectors that take advantage of the microtubules for a faster intracellular movement toward the nucleus. The protein proved to efficiently interact with and to condense pDNA, forming small positively charged particles. These are regarded as crucial features for effective non-viral gene delivery vectors and may contribute to the T-Rp3 performance during transfection. Transfection assays using HeLa cells showed that T-Rp3 is a very efficient delivery vehicle, even when compared with Lipofectamine 2000™, presenting a reduced cytotoxicity. The confocal microscopy studies indicated fast perinuclear accumulation of pDNA following transfection, co-localizing with dense concentrations of microtubules. The results presented here strongly indicate that the cell microtubule network plays an important role in the trafficking of pDNA:T-Rp3 particles. However, due to the complex nature of these vectors and the diversity of cellular entry pathways and intracellular trafficking, investigating the pDNA:T-Rp3 routes inside the cells is a very challenging tasks. Vectors may rely on the microtubule network by different forms, including direct or indirect interaction and also transport inside endocytic vesicles. These different intracellular routes may also happen as parallel events. The detailed understanding of the mechanisms involved in the intracellular trafficking of modular protein vectors is one of the major goals of our group and the studies are still in progress. Taken together, the results presented here indicate that the strategy of exploiting dynein light chains for the design of modular recombinant proteins is promising and may significantly contribute to the development of more efficient non-viral gene delivery vectors.

Acknowledgments

The authors gratefully acknowledge the financial support of the Fundação de Amparo à Pesquisa do Estado de São Paulo – FAPESP (São Paulo, Brazil, Grant 2007/58323-9) and Conselho Nacional de Desenvolvimento Científico e Tecnológico – CNPq (Brazil, Grant 471971/2011-1). We also thank the Laboratório de Espectroscopia e Calorimetria (LEC), Laboratório Nacional de Biociências – LNBio (Campinas, Brazil), and the National Institute of Science and Technology on Photonics Applied to Cell Biology (INFABIC), UNICAMP, for the support for the analysis of recombinant T-Rp3. Finally, we thank Professor Maricilda Palandi de Mello, CBMEG, UNICAMP (Campinas, Brazil), for support for the HeLa cell culture.

Appendix A. Supplementary data

Supplementary data associated with this article can be found, in the online version, at http://dx.doi.org/10.1016/j.jbiotec.2014.01.001.

References

Akita, H., Ito, R., Khalil, I.A., Futaki, S., Harashima, H., 2004. Quantitative three-dimensional analysis of the intracellular trafficking of plasmid DNA transfected by a nonviral gene delivery system using confocal laser scanning microscopy. Mol. Ther. 9, 443–451.

Azzoni, A.R., Ribeiro, S.C., Monteiro, G.A., Prazeres, D.M.F., 2007. The impact of polyadenylation signals on plasmid nuclease-resistance and transgene expression. J. Gene Med. 9, 392–402.

Barbar, E., Kleinman, B., Imhoff, D., Li, M., Hays, T.S., Hare, M., 2001. Dimerization and folding of LC8, a highly conserved light chain of cytoplasmic dynein. Biochemistry 40, 1596–1605.

Brewer, L.R., 1999. Protamine-induced condensation and decondensation of the same DNA molecule. Science 286, 120–123.

Brooks, H., Lebleu, B., Vives, E., 2005. Tat peptide-mediated cellular delivery: back to basics. Adv. Drug Deliv. Rev. 57, 559–577.

Dodding, M.P., Way, M., 2011. Coupling viruses to dynein and kinesin-1. EMBO J. 30, 3527–3539.

Douglas, M.W., 2004. Herpes simplex virus type 1 capsid protein VP26 interacts with dynein light chains RP3 and Tctex1 and plays a role in retrograde cellular transport. J. Biol. Chem. 279, 28522–28530.

Döhner, K., Nagel, C.-H., Sodeik, B., 2005. Viral stop-and-go along microtubules: taking a ride with dynein and kinesins. Trends Microbiol. 13, 320–327.

Edelstein, M.L., Abedi, M.R., Wixon, J., 2007. Gene therapy clinical trials worldwide to 2007 – an update. J. Gene Med. 9, 833–842.

Erazo-Oliveras, A., Muthukrishnan, N., Baker, R., Wang, T.-Y., Pellois, J.-P., 2012. Improving the endosomal escape of cell-penetrating peptides and their cargos: strategies and challenges. Pharmaceuticals 5, 1177–1209.

Ferrer-Miralles, N., Vázquez, E., Villaverde, A., 2008. Membrane-active peptides for non-viral gene therapy: making the safest easier. Trends Biotechnol. 26, 267–275.

Freitas, S.S., Azzoni, A.R., Santos, J.A.L., Monteiro, G.A., Prazeres, D.M.F., 2007. On the stability of plasmid DNA vectors during cell culture and purification. Mol. Biotechnol. 36, 151–158.

Ganta, S., Devalapally, H., Shahiwala, A., Amiji, M., 2008. A review of stimuli-responsive nanocarriers for drug and gene delivery. J. Control. Release 126, 187–204.

Gump, J.M., Dowdy, S.F., 2007. TAT transduction: the molecular mechanism and therapeutic prospects. Trends Mol. Med. 13, 443–448.

Hall, J., Karplus, P.A., Barbar, E., 2009. Multivalency in the assembly of intrinsically disordered dynein intermediate chain. J. Biol. Chem. 284, 33115–33121.

Holzbaur, E.L., Vallee, R.B., 1994. Dyneins: molecular structure and cellular function. Annu. Rev. Cell Biol. 10, 339–372.

Kamiya, H., Fujimura, Y., Matsuoka, I., Harashima, H., 2002. Visualization of intracellular trafficking of exogenous DNA delivered by cationic liposomes. Biochem. Biophys. Res. Commun. 298, 591–597.

Kay, M.A., 2011. State-of-the-art gene-based therapies: the road ahead. Nat. Rev. Genet. 12, 316–328.

King, S.M., 2000. The dynein microtubule motor. Biochim. Biophys. Acta 1496, 1–16.

Lo, K.W.H., 2004. The 8-kDa dynein light chain binds to p53-binding protein 1 and mediates DNA damage-induced p53 nuclear accumulation. J. Biol. Chem. 280, 8172–8179.

Lukacs, G.L., Haggie, P., Seksek, O., Lechardeur, D., Freedman, N., Verkman, A.S., 2000. Size-dependent DNA mobility in cytoplasm and nucleus. J. Biol. Chem. 275, 1625–1629.

Lv, H., Zhang, S., Wang, B., Cui, S., Yan, J., 2006. Toxicity of cationic lipids and cationic polymers in gene delivery. J. Control. Release 114, 100–109.

Makokha, M., Hare, M., Li, M., Hays, T., Barbar, E., 2002. Interactions of cytoplasmic dynein light chains Tctex-1 and LC8 with the intermediate chain IC74. Biochemistry 41, 4302–4311.

Mastrobattista, E., van der Aa, M.A.E.M., Hennink, W.E., Crommelin, D.J.A., 2006. Artificial viruses: a nanotechnological approach to gene delivery. Nat. Rev. Drug Discov. 5, 115–121.

Medina-Kauwe, L.K., Xie, J., Hamm-Alvarez, S., 2005. Intracellular trafficking of non-viral vectors. Gene Ther. 12, 1734–1751.

Mesika, A., Kiss, V., Brumfeld, V., Ghosh, G., Reich, Z., 2005. Enhanced intracellular mobility and nuclear accumulation of DNA plasmids associated with a karyophilic protein. Hum. Gene Ther. 16, 200–208.

Moschos, S.A., Jones, S.W., Perry, M.M., Williams, A.E., Erjefalt, J.S., Turner, J.J., Barnes, P.J., Sproat, B.S., Gait, M.J., Lindsay, M.A., 2007. Lung delivery studies using siRNA conjugated to TAT(48–60) and penetratin reveal peptide induced reduction in gene expression and induction of innate immunity. Bioconjug. Chem. 18, 1450–1459.

Moseley, G.W., Leyton, D.L., Glover, D.J., Filmer, R.P., Jans, D.A., 2010. Enhancement of protein transduction-mediated nuclear delivery by interaction with dynein/microtubules. J. Biotechnol. 145, 222–225.

Nitin, N., LaConte, L., Rhee, W.J., Bao, G., 2009. Tat peptide is capable of importing large nanoparticles across nuclear membrane in digitonin permeabilized cells. Ann. Biomed. Eng. 37, 2018–2027.

Ruponen, M., Arkko, S., Urtti, A., Reinisalo, M., Ranta, V.-P., 2009. Intracellular DNA release and elimination correlate poorly with transgene expression after non-viral transfection. J. Control. Release, 1–6.

Said Hassane, F., Saleh, A.F., Abes, R., Gait, M.J., Lebleu, B., 2009. Cell penetrating peptides: overview and applications to the delivery of oligonucleotides. Cell. Mol. Life Sci. 67, 715–726.

Spagnou, S., Miller, A.D., Keller, M., 2004. Lipidic carriers of siRNA: differences in the formulation, cellular uptake, and delivery with plasmid DNA. Biochemistry 43, 13348–13356.

Sugita, T., Yoshikawa, T., Mukai, Y., Yamanada, N., Imai, S., Nagano, K., Yoshida, Y., Shibata, H., Yoshioka, Y., Nakagawa, S., Kamada, H., Tsunoda, S.-I., Tsutsumi, Y., 2009. Comparative study on transduction and toxicity of protein transduction domains. Br. J. Pharmacol. 153, 1143–1152.

Suh, J.J., Wirtz, D.D., Hanes, J.J., 2003. Efficient active transport of gene nanocarriers to the cell nucleus. Proc. Natl. Acad. Sci. U.S.A. 100, 3878–3882.

Toledo, M.A.S., Favaro, M.T.P., Alves, R.F., Santos, C.A., Beloti, L.L., Crucello, A., Santiago, A.S., Mendes, J.S., Horta, M.A.C., Aparicio, R., Souza, A.P., Azzoni, A.R., 2013. Characterization of the human dynein light chain Rp3 and its use as a

non-viral gene delivery vector. Appl. Microbiol. Biotechnol., http://dx.doi.org/10.1007/s00253-013-5239-5.
Toledo, M.A.S., Janissen, R., Favaro, M.T.P., Cotta, M.A., Monteiro, G.A., Prazeres, D.M.F., Souza, A.P., Azzoni, A.R., 2012. Development of a recombinant fusion protein based on the dynein light chain LC8 for non-viral gene delivery. J. Control. Release 159, 222–231.
Tzfira, T., 2006. On tracks and locomotives: the long route of DNA to the nucleus. Trends Microbiol. 14, 61–63.
Vázquez, E., Ferrer-Miralles, N., Villaverde, A., 2008. Peptide-assisted traffic engineering for nonviral gene therapy. Drug Discov. Today 13, 1067–1074.
Williams, J.C., 2005. Crystal structure of dynein light chain TcTex-1. J. Biol. Chem. 280, 21981–21986.
Won, Y.-W., Lim, K.S., Kim, Y.-H., 2011. Intracellular organelle-targeted non-viral gene delivery systems. J. Control. Release, 1–11.
Yamano, S., Dai, J., Yuvienco, C., Khapli, S., Moursi, A.M., Montclare, J.K., 2011. Modified Tat peptide with cationic lipids enhances gene transfection efficiency via temperature-dependent and caveolae-mediated endocytosis. J. Control. Release 152, 278–285.
Zhang, S., Zhao, B., Jiang, H., Wang, B., Ma, B., 2007. Cationic lipids and polymers mediated vectors for delivery of siRNA. J. Control. Release 123, 1–10.